Adult human hepatocyte organoid expansion for in vitro testing and in vivo engraftment

Shannon Nicole Mitchell

A dissertation

submitted in partial fulfillment of

the requirements for the degree of

Doctor of Philosophy

University of

Washington 2024

Reading Committee:

Kelly R. Stevens, Chair

Princess Imoukhuede

Marta Scatena

Program Authorized to Offer Degree:

Bioengineering

University of Washington

Abstract

Adult human hepatocyte organoid expansion for
in vitro testing and in vivo engraftment

Shannon Nicole Mitchell

Chair of the Supervisory Committee:
Kelly Stevens
Bioengineering

The liver, an intricate organ with over 500 distinct functions within the human body, possesses remarkable regenerative capabilities following injury or resection. Its pivotal role in detoxification heightens its importance in determining the body's resilience to harmful substances. However, the rapid dedifferentiation of hepatocytes, the liver's primary parenchymal cells, in ex vivo conditions presents a challenge, hindering studies on liver function and regeneration in humans. To overcome this limitation, we have developed optimized in vitro models utilizing adult human hepatocyte organoids, which serve as valuable tools for modeling liver physiology and tissue engineering. Through these models, we investigated the effects of various growth factors on hepatic function, elucidated hepatocyte proliferation mechanisms, and systematically analyzed cell heterogeneity. Leveraging magnetic-activated cell sorting, we

enhanced the functionality of hepatocyte organoids, prolonging their efficacy. We conducted in vivo implantation studies of human hepatocyte organoids, demonstrating their comparable functionality to freshly thawed hepatocytes. Notably, our organoids exhibited promising results in immunodeficient mouse models. Utilizing acute and chronic drug-induced liver injury models, our organoids suggest therapeutic potential in aiding patients' recovery from drug overdose. This innovative approach lays the groundwork for transitioning our hepatocyte organoid model toward clinical application, thereby advancing the prospect of utilizing these organoids as a therapeutic intervention for liver-related disorders.

Table of Contents

LIST OF FIGURES

LIST OF TABLES

Chapter 1. Introduction

The field of hepatology and regenerative medicine has witnessed remarkable advancements in recent years, with a particular focus on the development of novel tools and strategies to study and address liver-related diseases. Among these, hepatocyte organoids have emerged as a promising avenue, offering a unique platform for studying liver biology, modeling diseases, and exploring potential therapeutic interventions. Hepatocyte organoids, three-dimensional structures derived from primary human liver cells, have become a focal point of scientific inquiry, as they offer a nuanced platform for probing liver-related diseases and investigating potential treatments. Through a multi-faceted approach, we aim to unveil the full spectrum of possibilities that hepatocyte organoids offer to the field.

1.1 LIVER PHYSIOLOGY AND FUNCTION

The mature human liver is responsible for executing more than 500 essential functions, most of which are carried out by specialized liver cells known as hepatocytes. These hepatocytes display significant variations in their metabolic activities, which enable them to effectively distribute and handle the extensive functional responsibilities of the liver(1).

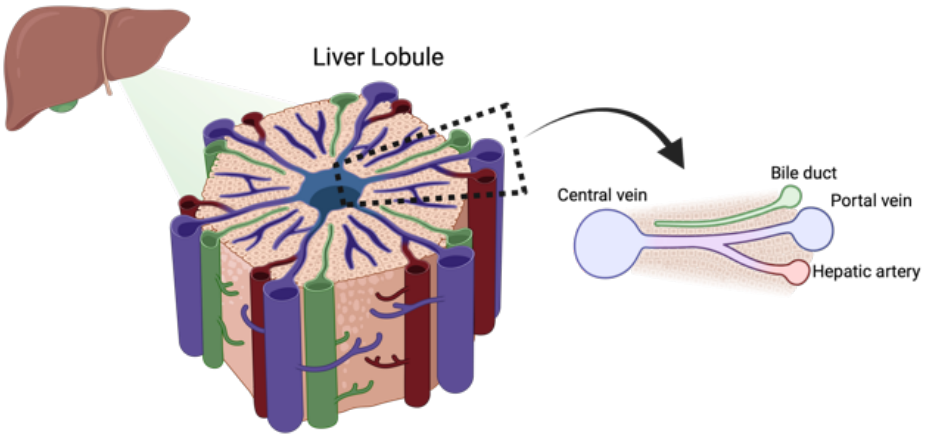

Figure 1.1: Adult Liver Structure (Adapted with permission from Sarah Saxton)

The liver's structure comprises lobes and smaller units called lobules. Within lobules, hepatocytes are arranged in rows radiating from a central point. The liver is endowed with a complex vascular system, including the hepatic artery, portal vein, and bile duct (2). The hepatic artery supplies oxygenated blood to the liver, ensuring that hepatocytes have the necessary oxygen for their metabolic processes (3). Simultaneously, the portal vein transports nutrient-rich, deoxygenated blood from the digestive tract. This abundant supply of oxygen and nutrients prompts portal hepatocytes to engage in energy-demanding tasks like protein synthesis and ureagenesis (4). The convergence of these two vascular systems forms an intricate network of sinusoids, which are highly permeable, thin-walled blood vessels that traverse the hepatic lobules. Sinusoids facilitate the exchange of nutrients and waste removal within the liver's functional units (5).

Within the hepatic lobules, the sinusoidal structure not only allows for the efficient exchange of nutrients but also plays a pivotal role in bile production (6). Hepatocytes, the liver's principal functional cells, secrete bile into tiny canaliculi. These canaliculi form an intricate network throughout the liver lobule and ultimately merge to form bile ducts (1,7) . This complex network of bile ducts conveys bile to the gallbladder for storage or directly to the small intestine for fat digestion (8,9).

The lining of the bile ducts, from the smallest canaliculi to the larger ducts, is composed of specialized epithelial cells called cholangiocytes (10). Cholangiocytes regulate the flow, composition and pH of the primary bile generated at the canaliculi of hepatocytes through different mechanisms, including the absorption of bile acids, glucose, and amino acids (step 1) and the secretion of bicarbonate and water (10,11).

The liver's extraordinary anatomical and physiological intricacies involve a highly specialized vascular system, intricate bile production, and meticulous control of digestive processes. These features underscore the liver's indispensable role in maintaining metabolic equilibrium and facilitating digestion in the human body.

1.2 LIVER REGENERATION

The inability of the liver to recover from many forms of damage and disease is somewhat surprising given the fact that the liver is a highly regenerative organ. For instance, in a partial hepatectomy, up to two-thirds of the liver can be surgically removed and the remaining liver mass can regrow over a matter of weeks, ultimately restoring the organ to its original size (12).

In animal models, such as rodents, partial hepatectomy involves a well-defined sequence of events, consisting of three main phases: priming, proliferation, and termination (13). The priming phase is initiated within the first hour of injury, although the precise trigger remains uncertain. One potential instigator may be hemodynamic overload, as the blood volume is confined to approximately 30% of the original vascular network (14). Research suggests that this abrupt blood volume and pressure alteration may induce the upregulation of stretch- or shear-induced angiocrine signals in liver sinusoidal endothelial cells (LSECs). These signals include molecules like hepatocyte growth factor (HGF), interleukin 6 (IL-6), and tumor necrosis factor (TNF), all of which are known to play roles in liver regeneration (14–16) . Vascular changes can also prompt the activation of matrix metalloproteinase 9 (MMP9) and urokinase plasminogen activator (uPA), initiating the remodeling of the liver's extracellular matrix and the release of matrix-bound growth factors like HGF and transforming growth factor-beta (TGF-β) (13,17,18) . Furthermore, the increased portal blood flow relative to the remaining liver mass enhances the

availability of portal factors such as epidermal growth factor (EGF), norepinephrine, insulin, bile acids, and serotonin. These factors can sensitize hepatocytes to other growth signals or directly stimulate cell cycle entry (19–22).

Chapter 2 lays the foundation for hepatocyte proliferation in liver regeneration. As we venture into Chapter 3, the focus shifts towards the intricate interplay of growth factors and their impact on hepatocyte growth and phenotype. Nevertheless, it remains evident that a multitude of enigmas persist regarding whether the majority of hepatocytes harbor the capacity for substantial proliferation. This question extends into our exploration of growth factors and their profound influence on hepatocyte the growth and phenotypic alterations.

1.3 ORGANOIDS

Organoids, often referred to as "mini-organs," provide a culture method capable of replicating the structure and function of a specific cell or organ when cultured under specific conditions involving media and matrix. A foundational reference to liver organoids dates back to Michalopoulos et al. in 1999 (23). However, Hans Clevers is frequently acknowledged as the pioneering figure in the modern organoid field, following his seminal paper that established human intestinal organoids derived from Lgr5+ intestinal stem cells (24). Clevers' groundbreaking discovery paved the way for the development of organoids derived from a multitude of cells and organs across the human body, ultimately earning organoids the distinction of being named "Method of the Year" by Nature Methods in 2017 (25).

Since the inception of Clevers' intestinal organoids, various hepatic organoid models have been created using diverse liver cell types at different stages of development. These models exhibit

varying degrees of similarity to human hepatocytes. The field has continued to evolve and expand its use of organoids, with the most recent advancements focused on the development of reliable and functional adult human hepatocyte organoids. The details of this progress will be elaborated upon in Chapters 3 and 4.

1.4 USE OF ORGANOIDS IN LIVER DISEASE

The liver plays a pivotal role in human metabolism, detoxification, and storage, making liver disease a profound threat to human health. This issue represents a pressing public health concern, as unlike many other leading causes of death, liver disease-related fatalities are escalating rather than declining (26,27). This rising trend compounds an already substantial public health burden, with liver disease accounting for more than 1.3 million annual global deaths (28). The causes of liver disease encompass genetic mutations (e.g., tyrosinemia, alpha-1 antitrypsin deficiency), viral infections (e.g., hepatitis), or other factors, including drugs or dietary factors (29). Acute liver failure, primarily resulting from acetaminophen (e.g., Tylenol, paracetamol) overdose, is the predominant reason for calls to Poison Control Centers and the leading cause of emergency liver transplantation among young adults (19,30). While some factors, such as drug overdoses, can lead to acute liver failure, the typical progression of liver disease involves the gradual deterioration of liver tissue over months to years (20). Chronic liver disease can be triggered by any of the previously mentioned causes, but recurring damage to the tissue eventually leads to a condition known as cirrhosis, characterized by severe scarring and impaired liver function (20). Cirrhosis is a precursor to liver failure and substantially elevates the risk of liver cancer (21).

Regrettably, treatment options for advanced liver disease remain quite limited, resulting in

significant global morbidity and mortality. Cirrhosis and liver cancer rank as the 11th and 16th leading causes of death worldwide, jointly accounting for 3.5% of global mortality (26). The only curative therapy for late-stage liver disease is a liver transplant; however, the demand for donor organs significantly surpasses their availability, with this gap widening annually (22,26,31). While whole-organ transplants can provide a cure for both acute and chronic liver failure, the increasing prevalence of liver disease implies a growing number of patients in need of transplants, even as the supply of donor organs remains relatively static (32–34). Furthermore, disparities in the United States exist concerning access to liver transplants, with Black and Latinx/Hispanic patients less likely to be referred for transplant evaluations, resulting in more advanced disease and poorer outcomes post-surgery (35–37). Women also face lower transplant rates while on the transplant waiting list (36). Collectively, 10-20% of patients die while awaiting a liver transplant (38). Hence, the exploration of alternative treatment modalities is of utmost importance in the context of alleviating the morbidity and mortality associated with liver disease. Our current research efforts are focused on evaluating various methodologies, including injections into the gondola fat pad and spleen, and the implantation of liver tissue seeds. These approaches all involve the utilization of human hepatocyte organoids, to assess their therapeutic efficacy in rescuing mice from liver injury and disease. This research seeks to determine whether these interventions can serve as either a transitional therapy or a viable alternative to whole organ transplantation, as discussed in Chapter 5, where a liver disease model for hereditary tyrosinemia I is presented, Chapter 6, which explores the use of these methods in cases of acetaminophen poisoning leading to acute liver failure, and Chapter 7, which examines their application in the context of CCl4-induced liver damage.

1.5 CONCLUSION

Addressing the global challenge of liver disease and paving the way for innovative solutions to prevent or reverse its progression, our research adopts an integrated approach that combines human organoid biology, cutting-edge technology, and pre-clinical animal modeling. This transformative method is used to revolutionize the procurement of hepatocyte cells and substantially expedite the development of therapeutic strategies for liver failure. Central to this approach is the need for a dependable and scalable hepatocyte population, essential for creating human liver models and advancing the field of cell-based therapies.

The studies presented in this thesis will unveil a novel therapeutic pathway for effectively treating both acute and chronic liver diseases, promising to have a profound impact on global public health.

Chapter 2. Hepatocyte proliferation *in vitro*

2.1 INTRODUCTION

Hepatocytes, the principal functional cells of the liver, are generally characterized by their quiescent state, meaning they remain largely dormant and do not actively engage in the cell cycle. However, they retain the inherent capacity to re-enter the cell cycle and undergo division under specific conditions. The study of hepatocyte proliferation has assumed significant importance in the realm of liver research due to its pivotal role in maintaining liver homeostasis and its potential relevance to various pathological conditions. *In vitro* studies of hepatocyte proliferation offer a valuable experimental platform, enabling a controlled and isolated examination of the factors that regulate the division of hepatocytes and manipulate and analyze cellular microenvironments(39–41). They provide a unique vantage point for exploring the intricate web of cell signaling pathways that orchestrate hepatocyte proliferation and systematically examine cell heterogeneity. By manipulating specific components of these pathways, researchers can decipher the key molecules and events that contribute to hepatocyte division.

2.2 RESULTS

Organoids are three-dimensional miniature organs grown *in vitro*, exclusively utilizing human hepatocytes sourced from adult patients and 3D matrix called Matrigel. They are cultured in conditions that mimic the human body for optimal liver morphology and phenotypes. Over time, the cells self-organize into three-dimensional structures, undergoing maturation and potential differentiation.

In previous studies, hepatocyte cultures expanded in *vitro* for a maximum duration of 14 days. We

sought to investigate the extent to which human hepatocyte organoids could be expanded, as detailed in Section 2.4. To gain a deeper understanding of hepatocyte proliferation, we employed a combination of techniques, including 5-ethynyl-2'-deoxyuridine (EdU) staining and immunofluorescence staining for hepatocyte markers such as Cytokeratin 18 (CK18), Cytokeratin 19 (CK19), and Hoechst. These analyses were conducted at two time points: Day 7 (Figure 2.1A) and Day 15 (Figure 2.1B).

Our data indicates a higher proliferation rate in human hepatocyte organoids at day 7 compared to day 14. By day 14, we observe a decrease in proliferative hepatocytes but mainly proliferative biliary cells, including cholangiocytes. To expand further on the cell proliferation rate over the time course of 14 days, we employed flow cytometry to quantitatively compare cell counts between the negative control and EdU-treated samples. Our single-cell data reveal the expression of cell cycle-related genes in a subset of hepatocytes during the initial week of growth but a higher proportion of proliferative cholangiocytes during the second week, as indicated by flow cytometry (Figure 2.1C-D). Our findings align with the reduction in proliferation observed over time, consistent with histological data.

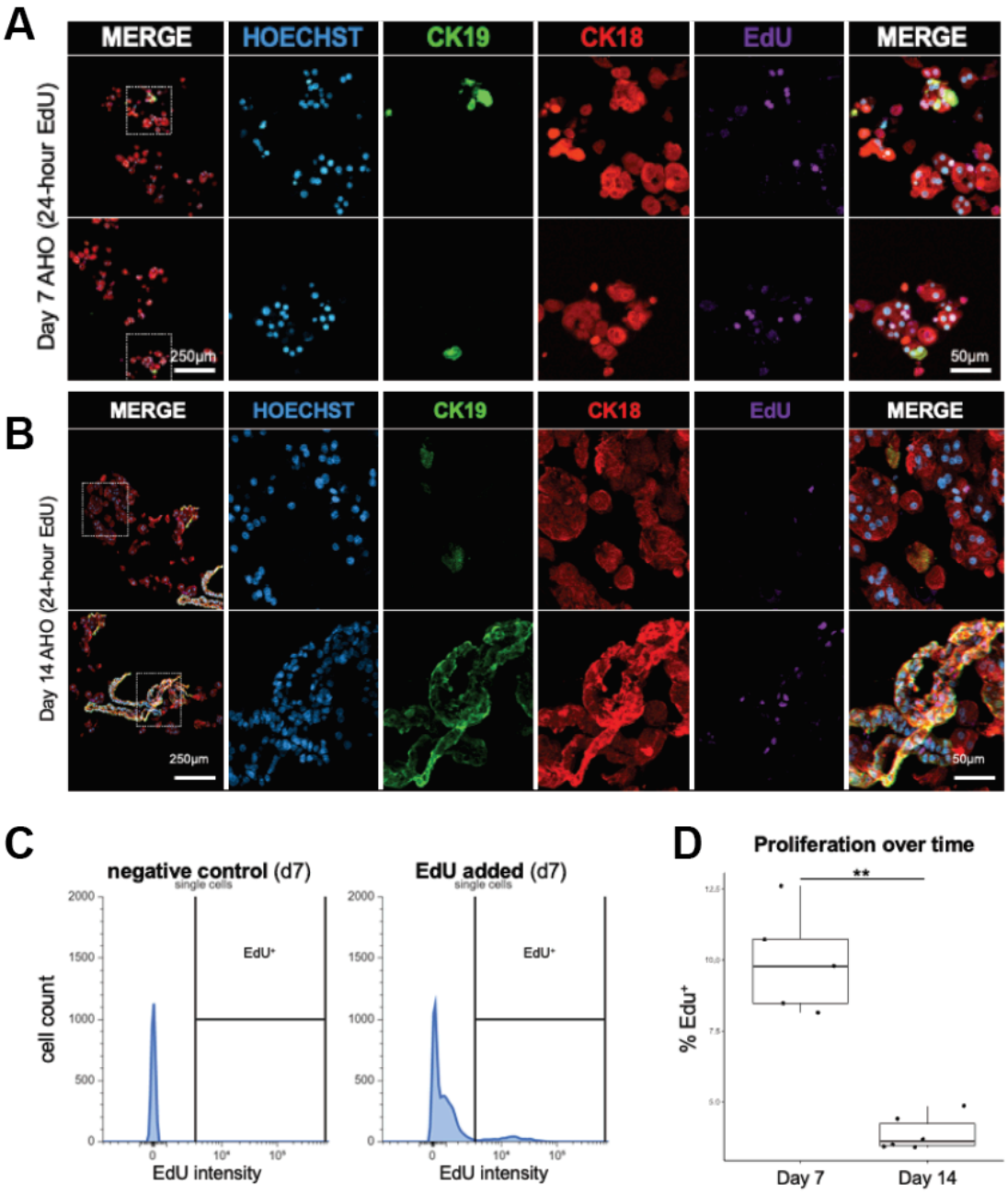

Figure 2.1: Human Hepatocyte Organoid Proliferation Over Time using EdU marker

(A) Immunofluorescence images of adult human hepatocyte organoids at day 7 for CK18 (red), CK19 (green), and Hoechst (blue). Scale bars = 250µm, merged image scale bar = 50µm

(B) Immunofluorescence images of adult human hepatocyte organoids at day 14 for CK18 (red), CK19 (green), and Hoechst (blue). Scale bars = 250µm, merged image scale bar = 50µm

(C) Cell Count for Adult Human Hepatocyte Organoids: A Comparative Analysis between EdU-Labeled and Unlabeled Samples

(D)Assessment of EdU Incorporation in Adult Human Hepatocyte Proliferation from Day 7 to Day 14 for Percentile Measurement.

We revisited previously obtained data once the proliferation reduction was confirmed through flow cytometry and histology. Single-cell RNA sequencing data unveiled a shift in the proliferative identity of cells between Day 5 (Figure 2.2A) and Day 15 of culture (Figure 2.2B). Notably, while hepatocytes remained proliferative at Day 5, cholangiocytes emerged as the primary proliferating cell type by Day 15, as indicated by their S and G2M scores. The top panel of our figures illustrates the differences in cell profiles between Day 5 and Day 15 separated into five distinct hepatocyte populations at day 5 (Figure 2.2A) and, one hepatocyte population, four cholangiocyte population and one mesenchymal cell population at day 15 (Figure 2.2 B). The bottom panel depicts the predicted cell cycle status based on single-cell data. The various cell cycle status predictions are represented by blue, indicating the S score (DNA synthesis), and orange, the G2M score (G2/Mitosis). Figures 2.2C and D demonstrate the gene expression of known markers for different cell types of the liver, demonstrating the changes in gene representation from day 5 to day 15 in the different cell type population.

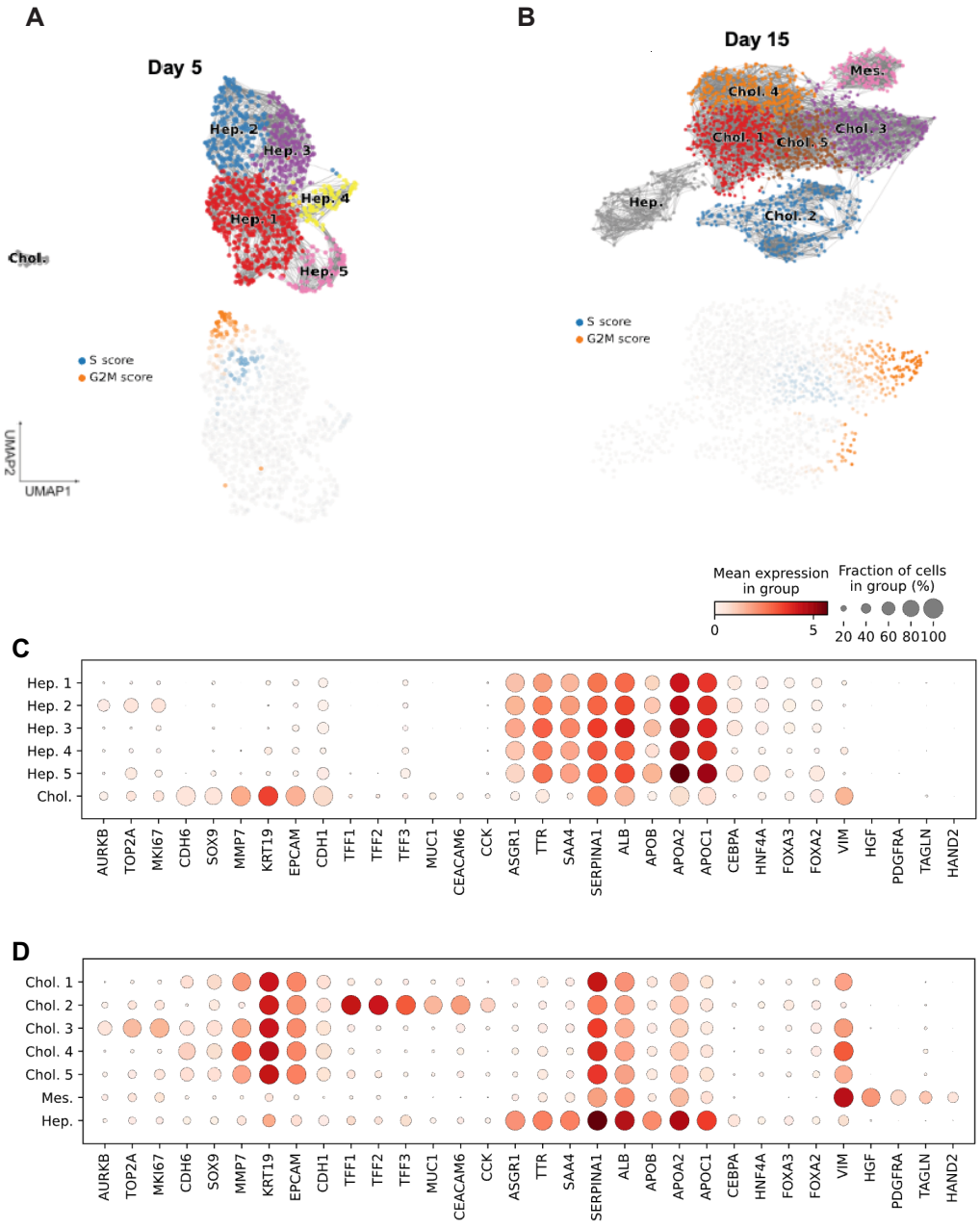

Figure 2.2: Alterations in Proliferative Patterns of Human Hepatocyte Organoids using Single-cell RNA Sequencing

(A) UMAP clustering of single cells from adult human hepatocyte organoids at day 5 in culture.

(B) UMAP clustering of single cells from adult human hepatocyte organoids at day 15 in culture

(C) Dot plot demonstrating average expression and percent of cells expressing genes of interest in each cluster from UMAP in (A). Genes selected as representative markers for different cell types of the liver

Dot plot demonstrating average expression and percent of cells expressing genes of interest in each cluster from UMAP in (B). Genes selected as representative markers for different cell types of the liver

2.3 DISCUSSION

The results of our study provide valuable insights into the expansion and proliferation dynamics of human hepatocyte organoids over a 14-day time course. The data from obtained histology, flow cytometry, and single-cell RNA sequencing consistently indicates that cell proliferation is more active on Day 7 versus Day 14; on Day 14, cholangiocytes proliferate but not hepatocytes. Previous research in our lab has predominantly focused on hepatocyte cultures expanded in vitro for a maximum duration of 14 days, while others suggest organoids can last up to 2-5 months while maintaining morphology and liver-specific functions (42). Our investigation aimed to extend this knowledge with a particular emphasis on understanding the dynamics of hepatocyte proliferation.

To analyze hepatocyte proliferation, a combination of techniques, including 5-ethynyl-2'-deoxyuridine (EdU) staining, immunofluorescence staining for Cytokeratin 19(CK19), Hoechst, and a hepatocyte marker such as Cytokeratin 18 (CK18), and single RNA sequencing. We conducted these analyses at two critical time points: Day 7 and Day 14 or 15 of the culture. EdU staining is a crucial method for identifying actively dividing cells within a tissue or cell culture and can be incorporated into replicating DNA during cell division (43). By quantifying the number of EdU-positive cells, we can estimate the proportion of cells undergoing active proliferation within the tissue or culture. However, it is essential to note that EdU has its limitations, particularly concerning polyploid cells (44). By showing cell division and not the entire cell cycle, it is unclear if cells are completing the cell cycle (43–45)with EdU not having the ability to conclusively show that we can only use this as a marker to assume proliferative activity.

Our data revealed an interesting trend in hepatocyte proliferation over the 14 days. On Day 7, we observed a higher rate of proliferation, primarily within the hepatocyte population, while in contrast, by Day 14, there was a more substantial presence of proliferative biliary cells, including cholangiocytes. This shift in proliferative cell types underscores the dynamic nature of the organoid culture system. It suggests that hepatocyte proliferation wanes as cholangiocytes become more prominent, consistent with histology data obtained. Studies have also shown that independently of proliferation, hepatocyte-to-cholangiocyte conversion occurs through transdifferentiation (46).

We employed flow cytometry to compare cell counts between negative control and EdU-treated samples to gain a quantitative understanding of these proliferation dynamics. Flow cytometry is advantageous for quantifying proliferation dynamics through EdU incorporation as it enables precise, quantitative analysis of individual cells in suspension. It offers multiparametric capabilities, simultaneously measuring various cellular parameters (47–49). However, this technique is sensitive to changes in antigen expression during different treatments, necessitating rigorous consideration of experimental variables like time after treatment, dosage, and patient characteristics (48,50). The utilization of flow cytometry in this study provides a robust and detailed approach for quantifying proliferation dynamics. However, careful attention to potential factors, such as antigen expression variations, is crucial to ensure the reliability and interpretation of the results.

To further characterize the changes in cellular proliferation, we revisited the single-cell RNA (scRNA) sequencing data. This analysis revealed a pronounced shift in the proliferative identity of cells between Day 5 and Day 14 of culture. Notably, while hepatocytes remained proliferative at Day 5, cholangiocytes became the primary proliferating cell type by Day 15, as evidenced by their S and G2M scores. The observed differences in cell profiles between these time points highlight the dynamic nature of the organoid culture system. Using scRNA sequencing, the limitations of EdU staining on polyploidy were resolved. Obtaining the G2M and S scores in conjugation with the EdU staining allows differentiation of cell division and polyploidy. These findings align with the overall reduction in proliferation observed over time, as confirmed through flow cytometry and histological analyses.

In conclusion, our study provides comprehensive insights into human hepatocyte organoids' expansion and proliferation dynamics over a maximum of 15 days. The combination of histological, flow cytometry, and single-cell RNA sequencing data supports the notion of a temporal shift in proliferative cell types within the culture. These findings have important implications for understanding hepatocyte biology and may contribute to developing more effective in vitro models for studying liver physiology and disease. Further work will explore functional implications of these observed changes in cell proliferation within human hepatocyte organoids and find techniques to confirm the differences in transdifferentiated versus proliferated cells.

2.4 METHODS

2.4.1 *Organoid culture of hepatocytes*

Cryopreserved hepatocytes were thawed into 37°C medium and quickly spun down at 70 x g. Cells were mixed with 45% organoid media and 55% Matrigel and seeded in 20 µl droplets in each well of 48-well plates. After Matrigel had solidified, 200 µl of organoid medium was added to each well. Organoid medium: 40% Basal medium (DMEM/F12, 1x GlutaMAX, 1x HEPES, 1x penicillin-streptomycin, 2% B27, 10 mM nicotinamide, 1.25 mM N-acetyl cysteine, 10 nM gastrin), 50% Wnt3a conditioned medium, 10% Rspo1 conditioned medium, 50 ng/ml EGF, 5 µM A83-01, and 10 µM y-27632. Medium was refreshed every 2-3 days with care not to disturb the Matrigel droplet. Organoid size and growth were quantified from minimum intensity projections of brightfield z-stacks taken on a Nikon Eclipse Ti inverted high-resolution widefield microscope.

2.4.2 *Organoid digestion and barcoding*

Organoids were grown in Matrigel under mature human hepatocyte culture conditions for 5 or 15 days, as described above. At each timepoint, organoids were pooled and suspended in TrypLE (Thermo) for 20-30 minutes until they had digested to single cells. The single-cell suspension was mixed with 1% BSA to prevent clumping and sticking to tubes/tips. Immediately before partitioning, cells were filtered through a FlowMi Cell Strainer (Belart) to remove cell clumps and debris. Cells were counted then loaded into a 10X Chromium flow cell using the Single Cell 3' v3 kit. 10X genomics barcoding and library construction were performed according to manufacturer's recommendations and generated libraries from 2327 cells at day 5 and 3411 cells at day 15 in culture.

2.4.3 *Brightfield microscopy and morphometric analysis*

Brightfield z-stack images were taken in the center of each organoid well at multiple time points on a Nikon Eclipse Ti inverted high-resolution widefield microscope. Z-stacks were flattened into a single image using a minimum intensity projection (MinIP) with FIJI or Nikon NIS-Elements software. Organoid size and growth were quantified from MinIP images in ImageJ software and graphed with GraphPad Prism software.

2.4.4 *Organoid histology, immunofluorescent staining, and microscopy*

Organoids were harvested from Matrigel, fixed in 4% PFA at room temperature for 30 minutes, then embedded in HistoGel (VWR). For 2D histology, HistoGel pellets were dehydrated in ethanol, embedded in paraffin, and sectioned using a microtome (5-20mm sections). Immunofluorescence staining of organoids was performed by deparaffinizing sections, performing antigen retrieval, blocking with normal donkey serum for 1 hour at room temperature, then incubating with primary antibody overnight at 4°C. The following day, sections were washed with PBS-T and then incubated with secondary antibody + Hoechst 33342 (Thermo H3570) for 1 hour at room temperature, washed, and mounted with Fluoromount-G (Invitrogen). All antibody information is included in Table 1. Images were obtained using a Nikon Eclipse Ti inverted high-resolution widefield microscope or a Nikon A1R scanning confocal microscope. Images were processed using Adobe Photoshop or ImageJ software. For morphometric analyses, images were thresholded and pixels were measured using ImageJ software.

Table 1: Antibody information

Antibody	*Vendor/Product #*	*Species*	*Dilution*	*Specificity*	*Identification Marker*	*Wavelength Excitation (nm)*
Human cytokeratin-18	Dako M701029-2	Mouse	1:25	Human	Hepatocytes	
Cytokeratin-19	Abcam ab52625	Rabbit	1:100	Human, Mouse	Cholangiocytes	
Human albumin	Bethyl A80-129A	Goat	1:100	Human	Synthesized by hepatocytes and serves as a key blood plasma protein; Clinical marker for assessing liver function	
Arginase-1	Sigma HPA003595	Rabbit	1:200	Human	Liver specific enzyme involved in the urea cycle, it is a marker for liver metabolism and function	
MRP2	Thermo TA812520	Mouse	1:500		Liver excretion function	
HNF4a	Abcam ab201460	Rabbit	1:100	Human, Mouse, Rat	Transcription factor that regulates liver-specific gene expression including glycolysis, bile acid synthesis and drug metabolism. HNF4 alpha is crucial for hepatocyte differentiation and identity.	
Ecad	R&D AF748	Goat	1:100	Human, Mouse, Rat	Cell adhesion protein vital for maintaining hepatocyte structure and tissue organization	
Ki67	Abcam ab16667	Rabbit	1:500	Human, Mouse, Rat, Marmoset	Nuclear proliferation	
Goat anti-mouse 555	Invitrogen A21127	Goat	1:500			555
Donkey anti-mouse 555	Invitrogen A31570	Donkey	1:1000			555
Donkey anti-rabbit 594	Invitrogen A21207	Donkey	1:1000			594
Donkey anti-rabbit 647	Invitrogen A31573	Donkey	1:1000			647
Donkey anti-goat 488	Invitrogen A11055	Donkey	1:1000			488
Donkey anti-goat 647	Invitrogen A21447	Donkey	1:1000			647
Donkey anti-rat 488	Invitrogen A21208	Donkey	1:1000			488

2.1.1 *Single cell RNA sequencing and bioinformatics*

Libraries were sequenced using an Illumina NextSeq 2000. Reads were aligned to the human genome GRCh38-2020-A and counted with the 10X Cell Ranger pipeline version 6.1.1 (51). The day 5 organoid library generated 74,577 mean reads per cell with 1,320 median genes per cell. The day 15 organoid library generated 41,264 mean reads per cell with 2,296 median genes per cell. Cell Ranger outputs were loaded into R using the Seurat v4.0 package (52) bioinformatic analysis was performed following the recommended vignettes for data integration and clustering described by the Satija lab. First, cell filtering was performed on individual libraries to remove cells with >500 genes and >25% mitochondrial RNA content to exclude fragments and dying cells from analysis; 1849 and 2796 cells remained from days 5 and 15, respectively. Next, global-scaling normalization and highly variable feature selection were performed. Cells were assigned a cell cycle score, which was regressed during data scaling to lessen the influence of these genes from clustering and prevent cell cycle genes from masking variations in liver gene signatures between cells. Two integrated datasets were generated: an integrated day 5 and day 15 organoid sample, and an integrated sample of day 5 and day 15 organoids, a publicly available hepatoblast sample (ArrayExpress under accession E-MTAB-7189), and multiple human liver datasets (GEO under accession numbers GSM4808962 and GSM4808963, GSM4808967, GSM5615002, GSM5616004, GSM5616006, GSM4041154, and GSM4041159). Integrated datasets were scaled, principal component analysis was performed, followed by UMAP clustering, and gene expression was visualized to assign cluster identities to known liver cell types. All plots were generated using R Studio and the Seurat package.

2.1.2 *Statistics*

Statistical analyses were performed with an unpaired t-test with unequal variance (Welch's correction). $P < 0.05$ was considered statistically significant. Welch's correction is a modification of the independent samples t-test and used when comparing the means of two groups to determine of they are significantly different. This method is used to account ofr unequal variances ehrn comparing means of two groups, allowing for higher accuracy when there is assumption of equal variances may not be true.

Chapter 3. Growth Factor Composition Affects Adult Human Hepatocytes Organoid Phenotypes

3.1 INTRODUCTION

Hepatocyte growth and proliferation are influenced by a variety of growth factors including Hepatocyte Growth Factor (HGF), Fibroblast Growth Factor (FGF) in various isotypes, and Transforming Growth Factor Beta (TGF-β). In this section, we will explore the affects that these growth factors have on hepatocyte growth and maintaining liver function.

TGF-β, is a multifunctional cytokine peptide with implications in numerous biological and cellular processes. Its influence spans a wide spectrum, encompassing the regulation of cell proliferation, oncogenesis, angiogenesis, and immunomodulation(43). Scientists continuously scrutinize this complex peptide group, seeking to uncover its enigmatic facets, including its diverse isoforms and novel functions. TGF-β pathways are elicited by TGF-β ligands binding to two pivotal types of receptors, namely type 1 and type 2. These receptors are located within the lipid bilayer, bridging the gap between the extracellular matrix and the cytoplasm(43,44). TGF-β pathway can be categorized into two distinctive signaling modes: canonical and non-canonical. The canonical pathway denotes a SMAD (S-adenosyl methionine decarboxylase) 2/3 dependent pathway whereas the non-canonical pathway represents a non-SMAD dependent pathway.

In the canonical signaling pathway, SMAD proteins play a central role. TGF-β Receptor 2 initiates the phosphorylation of TGF-β Receptor 1 upon binding with the active TGF-β ligand (44). This phosphorylated TGF-β Receptor propagates phosphorylation to the SMAD 2/3 complex, ultimately leading to the activation of SMAD 4. Subsequently, the activated SMAD complex

translocates into the cell nucleus, where it orchestrates the transcription of target genes. In contrast, the non-canonical pathway is characterized by its interaction with various signaling cascades, including MAP Kinase, NF Kappa B, and PI3K ATK mTOR pathways(45). Additionally, several growth factors, including FGF and HGF are integral to the complex regulatory network of TGF-β signaling.

FGF and HGF play pivotal roles in mediating cell growth and differentiation. FGF is known for its involvement in angiogenesis and tissue repair, while HGF is a potent mitogen for hepatocytes and has been associated with liver regeneration(46,47). These growth factors interact with the TGF-β pathway to modulate cellular responses and regulate gene expression patterns.

A TGF-β inhibitor, A83-01, serves as an inhibitor of SMAD signaling and epithelial-to-mesenchymal transition (EMT) induced by TGF-β, blocking only canonical TGF-β pathways. It achieves this by upregulating Wnt3, a critical factor in the upregulation of Wnt signaling pathway (6) . This signaling pathway is crucial for cell proliferation, differentiation, and tissue regeneration. Wnt signaling can interact with other signaling pathways including Notch pathway and FGF pathway which can lead to unpredictable cellular responses and detrimental effects like tumorigenesis(48,49). A83-01's inhibitory action on TGF-β-induced EMT is of particular interest in studies aimed at maintaining robust hepatocyte morphology and phenotypes.

Leveraging this comprehensive understanding of the TGF-β signaling pathways and the interaction with growth factors such as FGF, HGF, and the TGF-β inhibitory molecule A83-01, we have conducted studies aimed at identifying optimal media compositions. These compositions, composed of growth factors and small molecules, are designed to promote the enhanced growth

of adult human hepatocytes while simultaneously preserving their robust morphology and phenotypes.

3.2 RESULTS

Seeking improved purity, functionality and consistency, growth factor composition screening was conducted; these growth factors included HGF, FGF7, FGF10, and the small molecule A83-01 (Table 1). Compared to the original Hepatoblast media (media condition 1) obtained from the Vallier lab at the University of Cambridge. The base media contains Advanced DMEM/F12 supplemented with HEPES, penicillin–streptomycin and GlutaMAX, 2% B27, 20 mM nicotinamide, 2 mM N-acetylcysteine, 50% WNT3A conditioned medium, 10% R-Spondin, 50 ng ml−1 EGF and 50 μM A83-01. We found that media 7 with lower levels of A83-01 and Media 9 with HGF, FGF10, and lower levels of A83-01 significantly promotes the growth of the organoids based on brightfield images (Figure 3.1A) and average organoid area (Figure 3.1B). Further functionality testing on the organoids showed that albumin levels are higher in both conditions, Media 7 and 9, in comparison to the other media conditions in which albumin levels were subsequently low or equal to zero (Figure 3.1C).

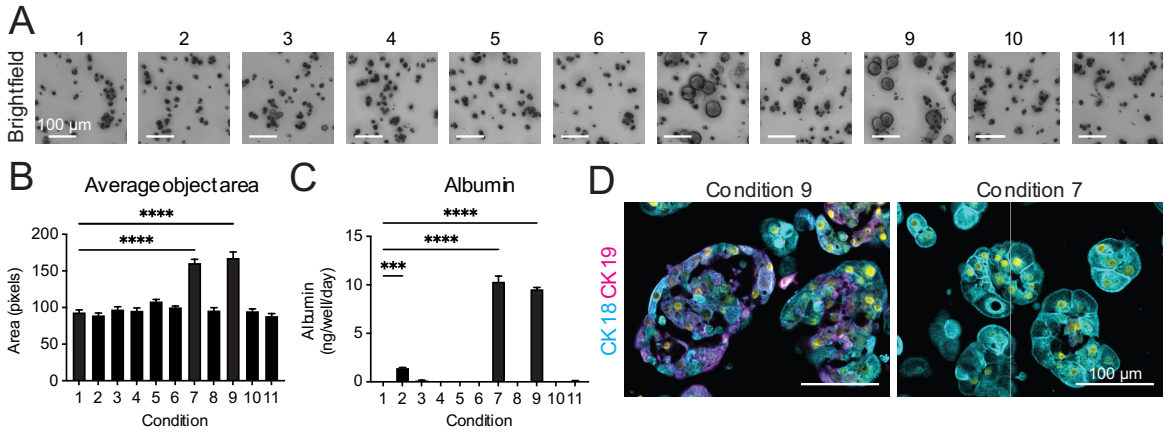

Table 2: Growth factor (GF) and small molecule (SM) Media Composition

Media	Base	HGF	FGF10	FGF7	5 µm A83-01	FGF1	FGF2
1	Base (with 50µm A83-01)						
2	Fetal hepatocyte	+	+	+	+		
3	No GF or SM						
4	Base	+					
5	Base		+				
6	Base			+			
7	Base				+		
8	Base	+	+	+			
9	Base	+	+		+		
10	Base					+	
11	Base						+

Figure 3.1: *In vitro* screening identifies optimal adult human hepatocyte organoid culture conditions

(A) Representative minimum intensity projections of brightfield z-stacks of adult human hepatocytes grown in 11 different culture conditions listed in Table 2. Scale bar = 100 µm.

(B) Average cross-sectional area of all cellular and multicellular objects in a single well at day 7. Data represented as mean +/- SEM of 16 wells. One-way ANOVA, Dunnett's multiple comparisons test, **** $p < 0.0001$.

(C) Albumin secretion measured by human albumin ELISA comparing adult human hepatocytes grown in 11 different media conditions listed in (E). Data represented as mean +/- SEM of 4 wells at day 9. One- way ANOVA, Dunnett's mltiple comparisons test, *** $p < 0.001$, **** $p < 0.0001$.

(D) Immunofluorescence images comparing adult human hepatocyte organoids grown in condition 9 (left) and condition 7 (right) stained for CK18 (cyan), CK19 (magenta), and Hoechst (yellow). Scale bar = 100 µm.

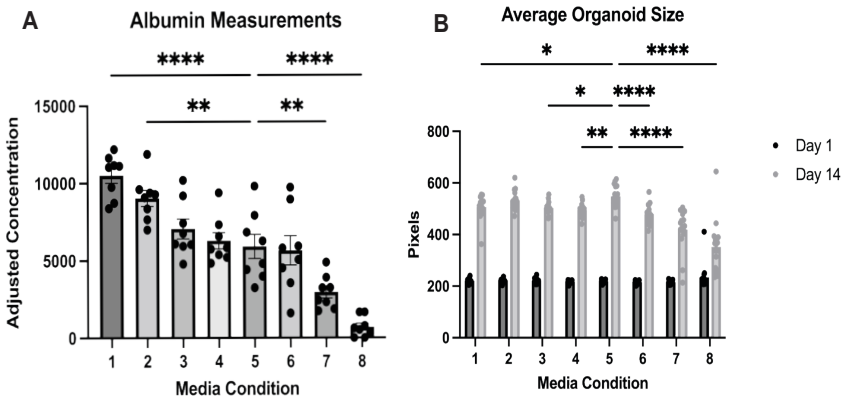

Table 3: A83-01 Titration Media Composition

Media	Concentration (μM)
1	0
2	0.5
3	1
4	2
5	5
6	10
7	20
8	50

Figure 3.2: *In vitro* screening identifies optimal A83-01 concentration for adult human hepatocyte organoid culture conditions

(A) Albumin secretion measured by human albumin ELISA comparing adult human hepatocytes grown in 8 different media conditions listed in Table 3. Data represented as mean +/- SEM of 4 wells at day 14. One- way ANOVA, Dunnett's multiple comparisons test.

(B) Average cross-sectional area of all cellular and multicellular objects in a single well at day 1 and day 14. Data represented as mean +/- SEM of 48 wells. One-way ANOVA, Dunnett's multiple comparisons test.

Based on this initial test, we sought to determine the levels of A83-01 for the optimal growth and functionality of organoids. To achieve this, a titration of A83-01 in the media 7 formulation was performed to determine the optimal concentration for hepatocyte organoid formation. Ultimately the lower concentration levels of A83-01 yielded higher human albumin levels (Figure 3.2A) and an increase in organoid size from day 1 to day 14 (Figure 3.2B). To expand on the impact of A83-01 and possible effects of TGF β inhibition and activation, low concentrations of A83-01, TGF Beta, and SB431542, an inhibitor of the actin receptor-like kinase (ALK), which ALK5 is the receptor related to the canonical TGF β signaling pathway were tested to determine what the optimal media formulation based on average organoid size at day 2 and day 14 (Figure 3.3A). We determined that TGF β activation was not beneficial compared to the inhibition of A83-01.

Our next study investigated the impact of different growth factor combinations on hepatocyte functionality and size when initiated with Basal Media, as described in Section 3.4.1. Specifically, we focused on the effects of Epidermal Growth Factor (EGF), Fibroblast Growth Factor (FGF), and Hepatocyte Growth Factor (HGF). The original media formulation contained 50 ng/mL of EGF. We assessed their effects using eight distinct growth factor conditions (Table 4) over a 15-day period. Notably, the addition of these growth factors led to significant alterations in the size of organoids (Figure 3.4B). Additionally, the human albumin ELISA results (Figure 3.4A) indicated significant results with the addition of only EGF in the Basal Media.

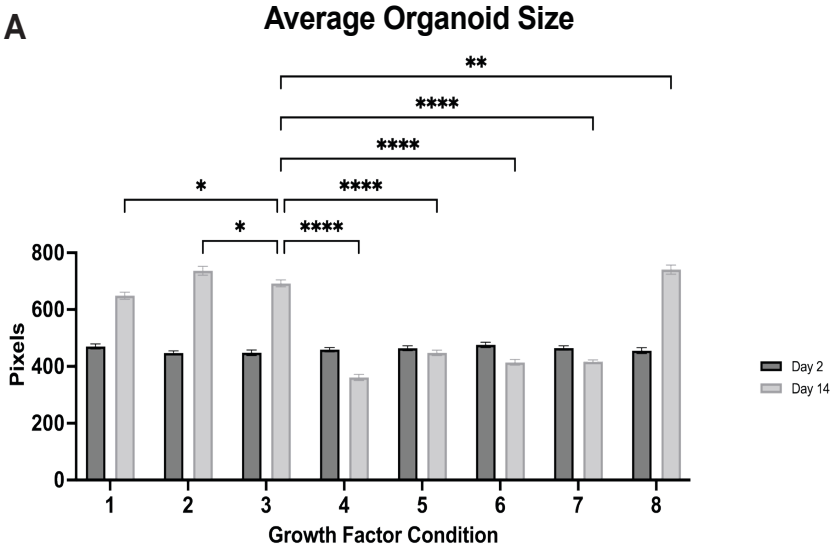

Table 4: A83-01, TGF-β and SB-431542 Media Composition

Media	Concentration (μM)
1	0μM A83-01
2	1μM A83-01
3	5μM A83-01
4	100μM A83-01
5	1nM TGF-β
6	10nM TGF-β
7	100nM TGF-β
8	SB431542

Figure 3.3: *In vitro* screening identifies optimal growth factor composition for adult human hepatocyte organoid culture conditions

(A) Average cross-sectional area of all cellular and multicellular objects in a single well at day 2 and day 14 comparing adult human hepatocytes grown in 8 different media conditions listed in Table 4. Data represented as mean +/- SEM of 48 wells. One-way ANOVA, Dunnett's multiple comparisons test.

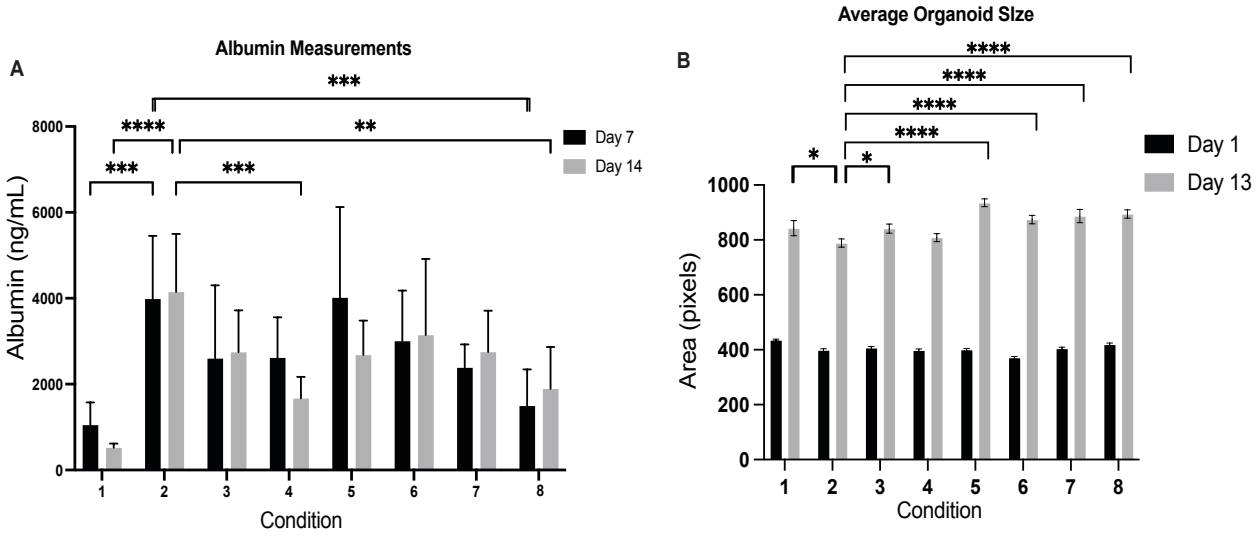

Table 5: Growth factor (GF) Media Composition using Basal Media

Media	Base	HGF	FGF1	EGF
1	Basal Media			
2	Basal Media			+
3	Basal Media	+		
4	Basal Media		+	
5	Basal Media	+		+
6	Basal Media		+	
7	Basal Media	+	+	
8	Basal Media	+	+	+

Figure 3.4: *In vitro* screening identifies a combination of growth factors suitable for adult human hepatocyte organoid culture conditions

(A) Albumin secretion measured by human albumin ELISA comparing adult human hepatocytes grown in 8 different media conditions listed in Table 5. Data represented as mean +/- SEM of 4 wells at days 7 and 14. One- way ANOVA, Dunnett's multiple comparisons test.

(B) Average cross-sectional area of all cellular and multicellular objects in a single well at day 1 and day 13 comparing adult human hepatocytes grown in 8 different media conditions listed in Table 5. Data represented as mean +/- SEM of 48 wells. One-way ANOVA, Dunnett's multiple comparisons test.

Furthermore, a prominent concern in hepatocyte organoid cultures is the occurrence of hepatocyte-to-cholangiocyte transdifferentiation. Despite initially seeding pure hepatocyte colonies, cholangiocytes emerged during the organoid growth period. Tumor Necrosis Factor

alpha (TNF-alpha) is a cytokine known to inhibit biliary production. To investigate this phenomenon, we examined the effects of different TNF-alpha concentrations (0 nM, 10 nM, and 100 nM) in Basal Media over 15 days. Our findings revealed higher albumin levels at 0 nM and 10 nM compared to 100 nM. Immunofluorescence staining demonstrated that cholangiocyte formation was more centralized at 0 nM, whereas at 10 nM, cholangiocytes were more evenly distributed throughout the samples.

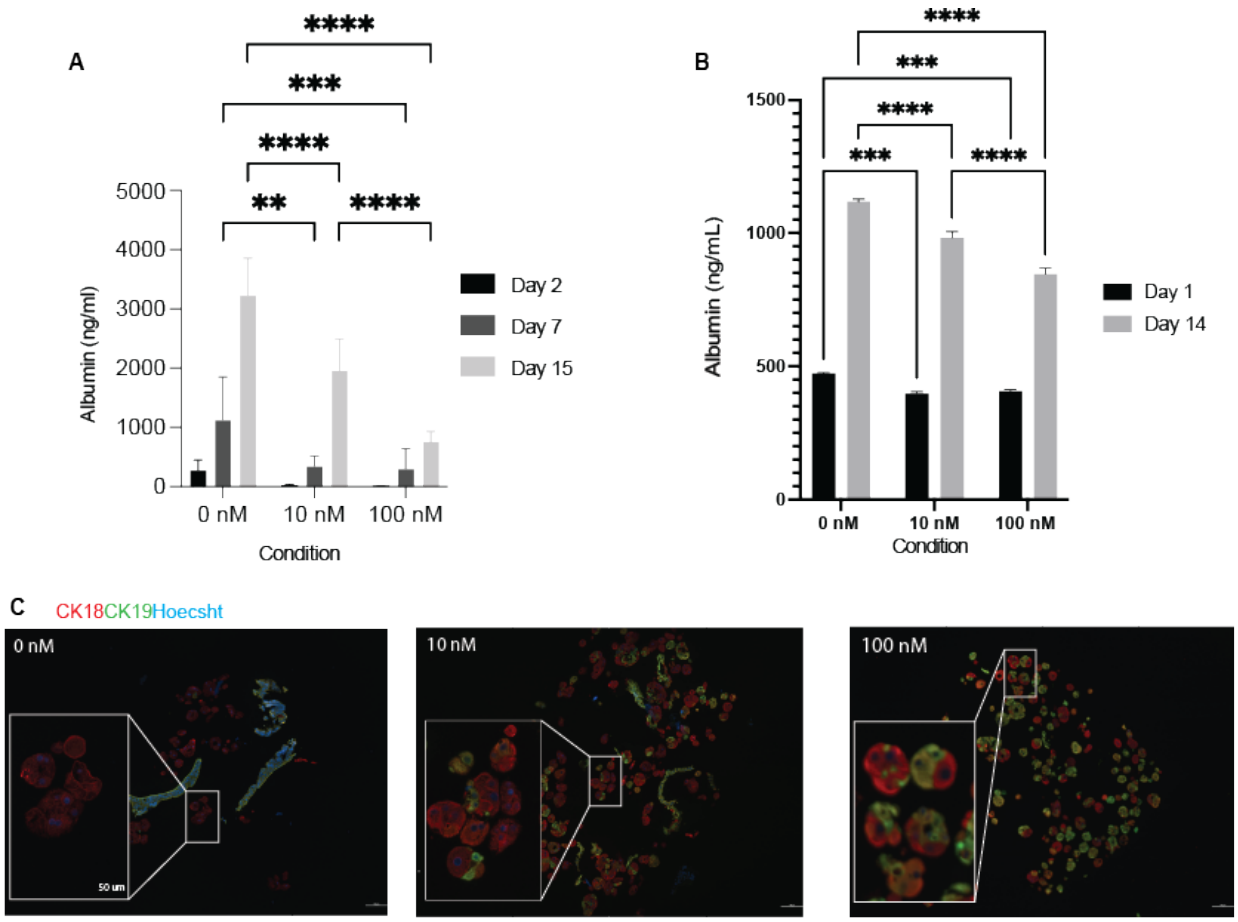

Figure 3.5: *In vitro* screening identifies a combination of growth factors suitable for adult human hepatocyte organoid culture conditions

(A) Albumin secretion measured by human albumin ELISA comparing adult human hepatocytes grown at 0, 10, and 100 nM TNF-Alpha. Data represented as mean +/- SEM of 4 wells at days 7 and 14. One- way ANOVA, Dunnett's multiple comparisons test.

(B) Average cross-sectional area of all cellular and multicellular objects in a single well at day 1 and day 14 comparing adult human hepatocytes grown. Data represented as mean +/- SEM of 48 wells. One-way ANOVA, Dunnett's multiple comparisons test.

(C) Immunofluorescence images comparing adult human hepatocyte organoids grown in 0nM TNF-alpha, 10 nM TNF-alpha (middle), and 100 nM (right)stained for CK18 (red), CK19 (green), and Hoechst (blue). Scale bar = 100 μm, inset scale bar = 50 μm.

3.3 DISCUSSION

Our primary objective was to refine the formulation of the culture medium to optimize the growth and functionality of adult human hepatocyte organoids. Optimizing the growth factor composition for organoid growth opens a new pathway for increased hepatocyte growth and culture longevity; we believe that the media composition is essential for hepatocyte growth and a decrease in hepatocyte to cholangiocyte transdifferentiation. The growth factors encompassed in this exploration include Hepatocyte Growth Factor (HGF), Fibroblast Growth Factor 7 (FGF7), Fibroblast Growth Factor 10 (FGF10), and a small molecule A83-01. These growth factors and small molecules were spotlighted; HGF is thought to be a pleiotropic factor influencing growth and regeneration and significant for hepatic mitigation as it stimulates epithelial cell proliferation, motility, morphogenesis, and angiogenesis in various organs via tyrosine phosphorylation of Met (53). The various FGF's tested are produced basally by the liver and shown to directly induce hepatocyte proliferation (54,55).

We commenced with the original hepatoblast media obtained from the Vallier lab at the University of Cambridge as our foundation for the formulation of organoid media. Through a comparison of various media formulations, as shown in Fig 1, we observed that Media 7, composed solely of low concentrations of A83-01, and Media 9, consisting of HGF, FGF10, and A83-01, played pivotal roles in facilitating the growth of these organoids. This is compared to Media 1, composed solely of high concentrations of A83-01, as evidenced by both brightfield images and the measurement of the average organoid area, where we saw significantly less hepatocyte proliferation and growth over time in Media 1 compared to Media 7 and 9.

Furthermore, our functional assessment of the organoids revealed substantially elevated levels of albumin in Media 7 and Media 9, compared to other media conditions, where albumin levels were either significantly lower or virtually nonexistent. Higher human albumin levels provide confirmation of the functionality of the adult human hepatocyte organoids. Specifically, the media formulations are more effective at supporting the hepatocyte-like characteristics serving as a confirmation of the organoid's enhanced functionality and viability with Media 7 and 9. These initial findings underscore the critical role of A83-01 in achieving optimal growth and functionality in hepatocyte organoids. A83-01 inhibits SMAD signaling and epithelial-to-mesenchymal transition by TGF-β induced upregulation of Wnt3.

Once we determined the importance of A83-01, to determine the optimal concentration, we chose 8 concentrations ranging from 0- 50 μM to titrate, keeping all other group conditions the same and in culture for 14 days. It was determined that the lower A83-01 concentrations performed better than the higher concentrations based on functionality testing of human albumin production and the quantification of average organoid size from day 1 to day 14. Striking, 0 μM of A83-01 was comparable to other concentrations of A83-01, making us question the role of TGF-β for optimal hepatocyte growth. To expand on this theory, concentrations of A83-01: 0, 1, 5 and 100μM, concentrations of TGF-β: 1, 10, and 100 nM and SB431542, an inhibitor of ALK5; receptor related to TGF-β were analyzed. Quantification of average organoid size concluded that higher concentrations of A83-01 and TGF-β activation did not play a significant role in adult human hepatocyte organoid formation, growth, and function. Based on the extensive growth factor testing conducted, we did see differences in which growth factor would impact hepatocyte growth, function, and phenotype. In Figure 3.2, the absence or minute concentration of 0.5 μM A83-01

proved to increase organoid size and hepatocyte function from human albumin levels. Consequently, Figure 3.3 proved that 1 uM A83-01 and SB431542 increased organoid size significantly, concluding that the inhibition of TGF β pathways are essential in the lifecycle of the adult human hepatocyte organoids .

Our subsequent study provides valuable insights into the impact of different growth factor combinations and the influence of Tumor Necrosis Factor alpha (TNF-alpha) on hepatocyte functionality, size, and the occurrence of hepatocyte-to-cholangiocyte transdifferentiation in hepatocyte organoid cultures.

Our study explored the effects of different growth factor combinations, specifically EGF, FGF, and HGF, when combined with Basal Media. Notably, we found that adding these growth factors resulted in significant alterations in the size of organoids. This suggests that the choice and concentration of growth factors play a crucial role in modulating hepatocyte organoid development. These findings align with previous research highlighting the importance of growth factors in influencing hepatocyte function and morphological characteristics. Moreover, our human albumin ELISA results indicated a significant increase in albumin production with the addition of only EGF in the Basal Media. This underscores the pivotal role of EGF in promoting hepatocyte-specific functions and the potential utility of EGF in hepatocyte culture systems. These findings provide a basis for further optimization of growth factor conditions in hepatocyte organoid cultures to enhance functional outcomes.

One of the challenges in hepatocyte organoid cultures is the emergence of cholangiocytes from initially seeded pure hepatocyte colonies. We investigated the effects of different TNF-alpha

concentrations (0 nM, 10 nM, and 100 nM) in Basal Media over a 15-day period. Our findings revealed higher albumin levels were observed at 0 nM and 10 nM TNF-alpha concentrations compared to 100 nM. This suggests that lower TNF-alpha concentrations may help maintain hepatocyte-specific functions, as elevated albumin levels indicate. Immunofluorescence staining provided additional insights, showing that cholangiocyte formation was more centralized at 0 nM TNF-alpha, while at 10 nM, cholangiocytes were more evenly distributed throughout the samples. This spatial distribution of cholangiocytes could affect the overall structure and function of hepatocyte organoids.

In summary, our research on growth factor media compositions provided valuable insights and established a foundational framework for future studies on optimizing organoid culture. Additionally, it highlighted the need for further analysis of factors influencing hepatocyte proliferation, phenotype, and function. Although the results did not yield significant differences that would warrant a change in the media formulation for subsequent studies, we decided to maintain the original formulation, including 5 µM of A83-01. As a result, we have concluded our media optimization investigations and will focus on other aspects of our research moving forward.

3.4 METHODS

3.4.1 *Organoid culture of hepatocytes*

Cryopreserved hepatocytes were thawed into 37°C medium and quickly spun down at 70 x g. Cells were mixed with 45% organoid media and 55% Matrigel and seeded in 20 µl droplets in each well of 48-well plates. After Matrigel had solidified, 200 µl of organoid medium was added to

each well. Organoid medium: 40% Basal medium (DMEM/F12, 1x GlutaMAX, 1x HEPES, 1x penicillin-streptomycin, 2% B27, 10 mM nicotinamide, 1.25 mM N-acetyl cysteine, 10 nM gastrin), 50% Wnt3a conditioned medium, 10% Rspo1 conditioned medium, 50 ng/ml EGF, 5 μM A83-01, and 10 μM y-27632. Medium was refreshed every 2-3 days with care not to disturb the Matrigel droplet. Organoid size and growth were quantified from minimum intensity projections of brightfield z-stacks taken on a Nikon Eclipse Ti inverted high-resolution widefield microscope.

3.4.2 *Brightfield microscopy and morphometric analysis*

Brightfield z-stack images were taken in the center of each organoid well at multiple timepoints on a Nikon Eclipse Ti inverted high-resolution widefield microscope. Z-stacks were flattened into a single image using a minimum intensity projection (MinIP) with FIJI or Nikon NIS-Elements software. Organoid size and growth were quantified from MinIP images in ImageJ software and graphed with GraphPad Prism software.

3.4.3 *Organoid histology, immunofluorescent staining and microscopy*

Organoids were harvested from Matrigel, fixed in 4% PFA at room temperature for 30 minutes, then embedded in HistoGel (VWR). For 2D histology, HistoGel pellets were dehydrated in ethanol, embedded in paraffin, and sectioned using a microtome (5-20mm sections). Immunofluorescence staining of organoids was performed by deparaffinizing sections, performing antigen retrieval, blocking with normal donkey serum for 1 hour at room temperature, then incubating with primary antibody overnight at 4°C. The following day, sections were washed with PBS-T and then incubated with secondary antibody + Hoechst 33342 (Thermo H3570) for 1 hour at room

temperature, washed, and mounted with Fluoromount-G (Invitrogen). All antibody information is included in Table 1. Images were obtained using a Nikon Eclipse Ti inverted high-resolution widefield microscope or a Nikon A1R scanning confocal microscope. Images were processed using Adobe Photoshop or ImageJ software. For morphometric analyses, images were thresholded and pixels were measured using ImageJ software.

3.4.4 *Albumin ELISA*

Organoid media was collected every 2-3 days and frozen. Secreted human albumin was then measured in media via enzyme linked immunosorbent assay (ELISA) using a goat anti-human albumin coating antibody and horseradish peroxidase-conjugated goat anti-human albumin detection antibody (Bethyl E80-129).

3.1.1 *Statistical Analysis*

Data in graphs are expressed as the mean ± SEM, as denoted in figure legends. Statistical significance was determined with PRISM software using *t*-test, one-way ANOVA, or two-way ANOVA followed by Sidak's, Dunnett's, or Tukey's multiple comparison test, as denoted in figure legends. These tests were used to compare multiple groups and determine which pairs are significantly different from each other. Sidak's test is used to control for familywise error rate while Dunnett's test is specifically designed for comparing multiple treatment groups against a single control group. Turkey's test compares all possible pairs of means and provides simultaneous confidence intervals. All of these tests serve a specific purpose in determining the significance of differences between group means.

Chapter 4. Purify hepatocyte organoid population using Magnetic-Activated Cell Sorting to prolong hepatocyte function *in vitro*

4.1 INTRODUCTION

Hepatocytes, the principal functional liver cells, are integral to various physiological processes, encompassing metabolism, detoxification, and protein synthesis, critically contributing to human homeostasis. Studying hepatocytes *in vitro* is essential for advancing our knowledge of liver function, disease modeling, drug development, and regenerative medicine. However, sustaining hepatocyte function in vitro remains challenging due to the limited lifespan of hepatocytes in traditional cell culture methods.

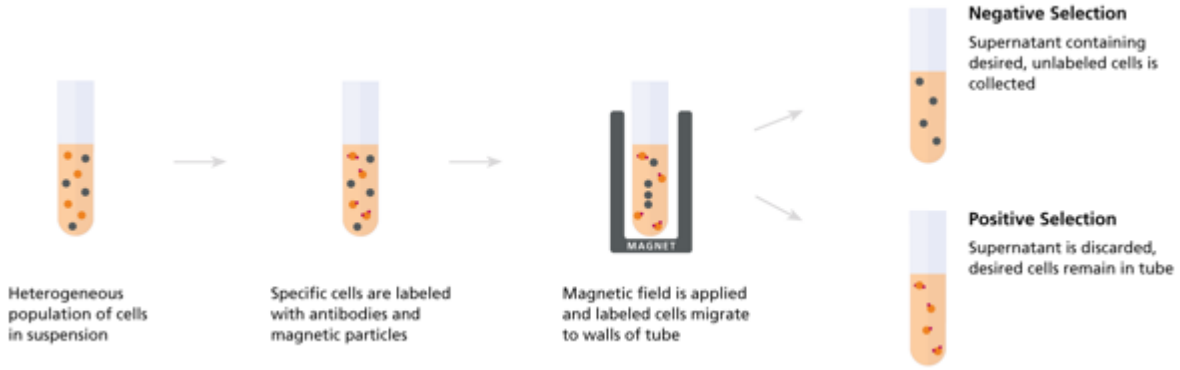

Figure 4.1: Negative and Positive Selection in a Column-Free Magnetic Cell Separation Technology STEMCELL Technologies(56)

Prolonging hepatocyte function *in vitro* has the potential to transform liver research and therapeutic development. Innovative strategies are being explored to address this challenge, with one such approach being to combine Magnetic-Activated Cell Sorting (MACS) and hepatocyte organoid cultures (Figure 4.1). MACS is a magnetic nanoparticle-based cell separation method that employs antibodies targeting specific surface markers (e.g., EPCAM for non-parenchymal cells in the liver such as cholangiocytes and stem cells) to selectively isolate and enrich hepatocytes within

organoids, minimizing the influence of non-parenchymal cells and enhancing their long-term viability and functionality(56,57).

This section introduces the concept of employing magnetic activated cell sorting to purify hepatocyte organoid populations, to extend their functional longevity in vitro. Despite the advantages of MACS and cell sorting, challenges may emerge over extended culture periods, such as gradual loss of hepatocyte-specific functions and dedifferentiation.

4.2 RESULTS

As shown in previous chapters, we have investigated the impact of various growth factors and media compositions on the long-term functionality of these adult human hepatocytes. In this section, we employed purification steps to evaluate their effectiveness in isolating non-parenchymal cells, such as biliary cells (cholangiocytes) from hepatocytes in adult human hepatocyte organoids. It was unclear whether the organoids needed to be subjected to rigorous dissociation, separating them into single cells to achieve better cell purification. In the first experiment, in order to determine which dissociation conditions yield better isolation of hepatocytes from organoids grown for 14 days, the organoids were subjected to passage procedures utilizing one of the three methods: (1) a 10-minute TrypLE treatment, (2) a 30-minute Cell Recovery Solution (Corning) treatment, or (3) a combination of both the 30-minute Cell Recovery Solution and the 10-minute TrypLE solution. Following this, organoids were subjected to labeling with EPCAM-positive and MACS beads (STEMCELL); the cells were separated using a magnet for 5 minutes, leading to the isolation of EPCAM-positive and negative cells in distinct reservoirs, subsequently resuspended in HBSS w 10mM HEPES with 2% fetal bovine serum (FBS).

The EPCAM-negative hepatocytes were plated into 42 wells, while the EPCAM-positive cells, mostly cholangiocytes, were plated into 6 wells of a 48-well plate. Subsequently, the organoids were monitored and imaged every 7 days, with harvest occurring at the 12-day mark post-passage. Brightfield images revealed reduced cholangiocyte growth in the EPCAM-negative group, whereas the EPCAM-negative group treated with TrypLE exhibited higher cell viability and diminished cholangiocyte growth (Figure 4.3A).

To determine which of the two MACS approaches, column-based Miltenyi vs. non-column-based Stemcell, would yield the most functionally active hepatocyte organoids, we compared Miltenyi vs. Stemcell in the next experiment. Our experiments showed that Miltenyi MACS sorted organoids had greater albumin levels (Figure 4.2B) and retained CK18, as shown in ELISA and immunostaining (Figure 4.2C), indicating that Miltenyi MACS resulted in improved hepatocyte enrichment.

In three different experiments, we noted that the decrease in albumin level over time occurred less when in the shorter culture of organoids, as shown in the comparison of albumin levels in organoids sorted after 14-day vs. 10-day vs. 7-day culture periods. These findings suggest that sorting after a 7-day culture may prolong hepatocyte function over long-term culture.

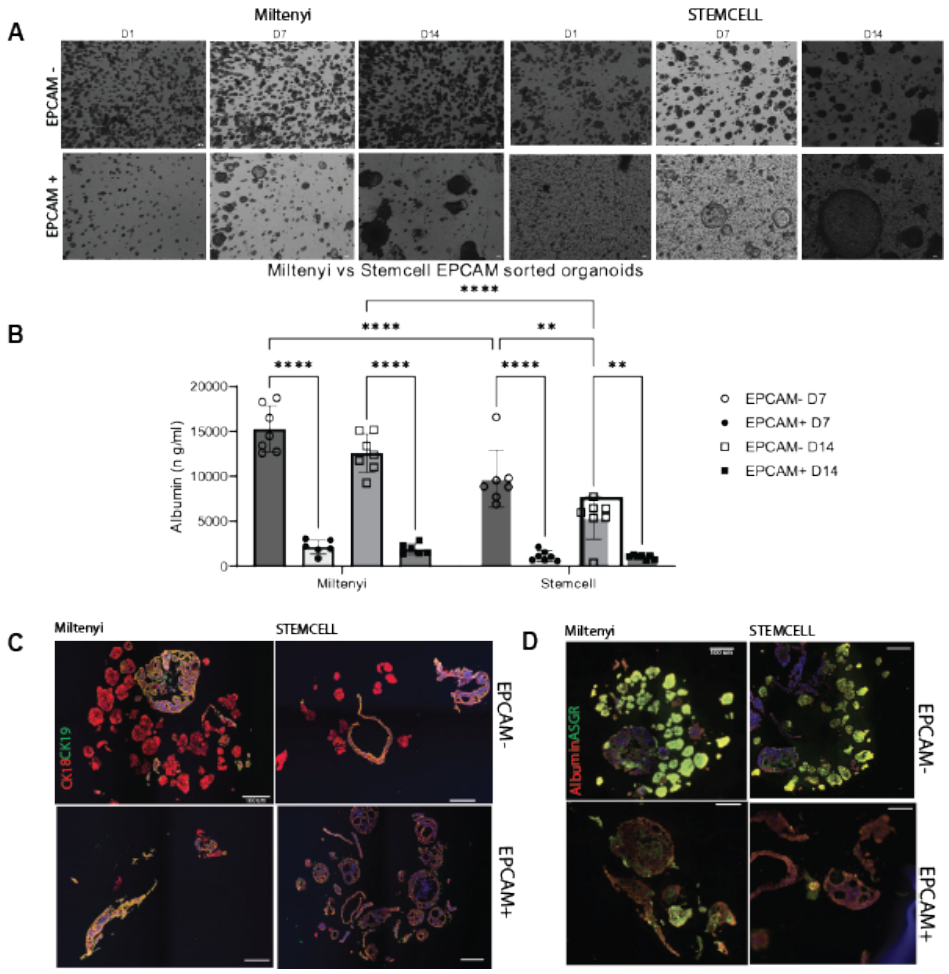

Figure 4.2: Sorting of Adult Human Hepatocyte Organoids Affects Hepatocyte Enrichment

(A) Representative minimum intensity projections of brightfield z-stacks of EPCAM positive and negative cells sorted using Miltenyi and STEMCELL separation methods Day 1, 7, and 14. Scale bar = 100 µm.

(B) Albumin secretion measured by human albumin ELISA comparing EPCAM positive and EPCAM negative adult human hepatocytes grown between Days 7 and 14 in conditions of Miltenyi and STEMCELL separation methods Data represented as mean +/- SEM of 48 wells. One-way ANOVA, Dunnett's multiple comparisons test.

(C) Immunofluorescence images comparing EPCAM positive, and EPCAM negative adult human hepatocyte organoids separated using Miltenyi and STEMCELL methods stained for CK18 (red) and CK19 (green). Scale bar = 100 µm.

(D) Immunofluorescence images comparing EPCAM positive, and EPCAM negative adult human hepatocyte organoids separated using Miltenyi and STEMCELL methods stained for Albumin (red) and ASGR (green). Scale bar = 100 µm.

To investigate the potential for sustained hepatocyte function under different conditions, we maintained organoids under the original growth conditions for 42 days, representing the control group. These organoids were divided and replated every 14 days, resulting in a decline in albumin levels over the 42-day timeframe (Figure 4.3C).

In response to this observed decline, we employed MACS, which revealed a substantial decrease in human albumin levels compared to the control group (Figure 4.3C). Further experimentation led us to attempt sorting and splitting organoids every 7 days during the initial 14 days, aiming to minimize the loss of cells as organoids tend to grow more effectively when clustered together (Figure 4.3B). The data indicated that organoids did not maintain their function after the second passage, likely due to excessive cell removal at day 28. Notably, we observed decreased human albumin production even when the passaging and sorting were halted at day 14. Nonetheless, compared to the control group, we observed a less pronounced decline in albumin levels.

In conclusion, our findings demonstrate that passaging and sorting at earlier time points positively contribute to the long-term functionality of adult human hepatocyte organoids. These results underscore the significance of cell purification techniques in enhancing the longevity and effectiveness of hepatocyte culture systems.

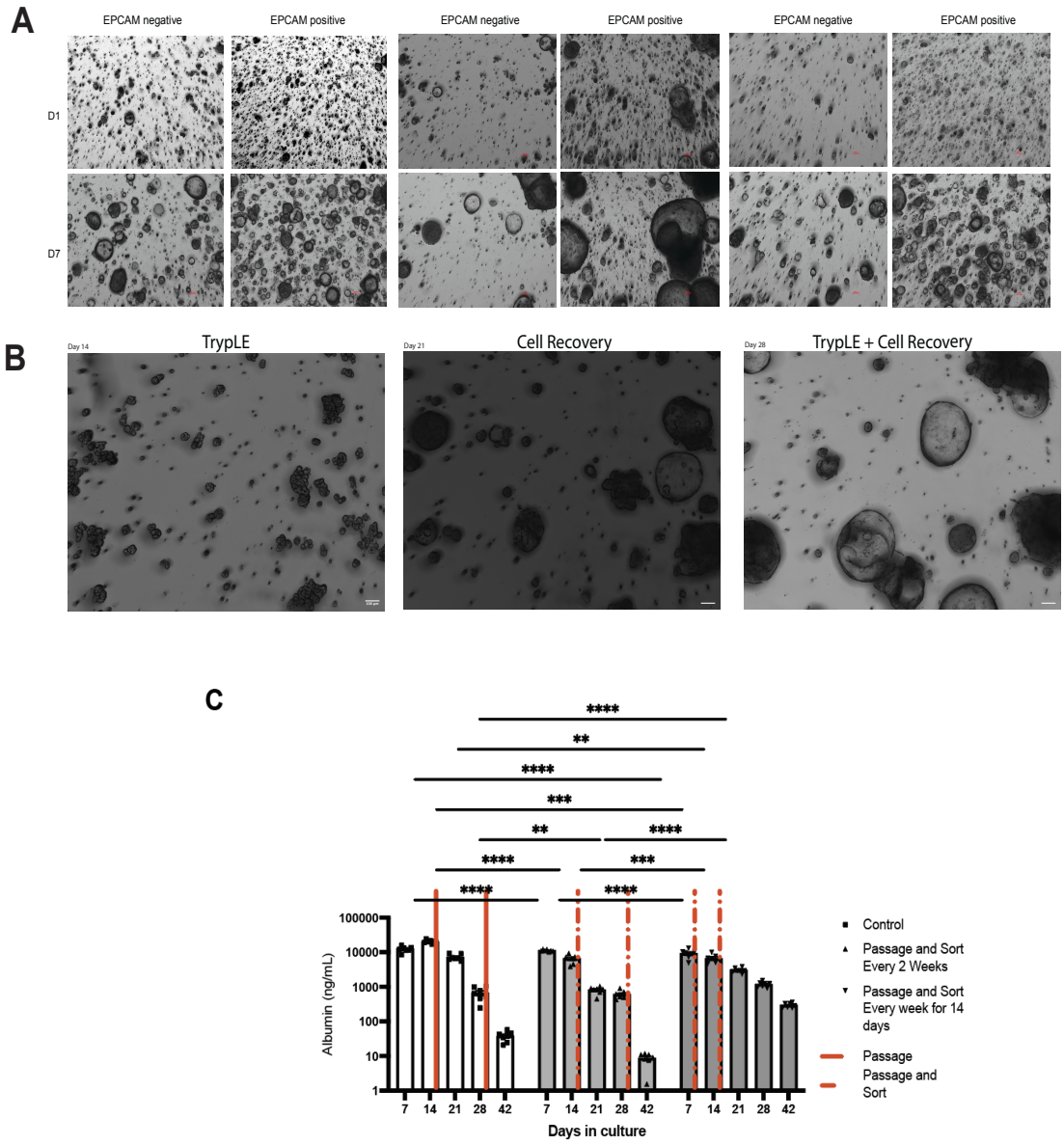

Figure 4.3: Passaging and Sorting of Adult Human Hepatocyte Organoids Affects Long Term Hepatocyte Functionality

(A) Representative minimum intensity projections of brightfield z-stacks of EPCAM positive and negative cells sorted in three different culture conditions at Day 1 and Day 7. Scale bar = 100 μm.

(B) Representative minimum intensity projections of brightfield z-stacks of sorted adult human hepatocytes at Day 14, 21, and 28. Scale bar = 100 μm.

(C) Albumin secretion measured by human albumin ELISA comparing adult human hepatocytes grown between Days 7 and 42 in conditions of: Control (black square) Passage and sort every 2 weeks (upright triangle) and Passage and sort every week for 14 days (upside down triangle). Data represented as mean +/- SEM of 4 wells. One-way ANOVA, Dunnett's multiple comparisons test

4.3 DISCUSSION

The results of this study shed light on the critical factors affecting the long-term functionality of adult human hepatocyte organoids and the significance of purification techniques in improving their viability. In the pursuit of these objectives, we carried out a series of experiments involving cell dissociation, labeling, and sorting methods. The following discussion highlights the key findings and their broader implications.

The primary focus of this study was to explore methods for effectively separating biliary cells (cholangiocytes) from hepatocytes within adult human hepatocyte organoids. In our study, we aimed to determine the most effective approach for the purification of hepatocyte organoids by comparing two magnetic-activated cell sorting (MACS) methods: the column-based Miltenyi system and the non-column-based STEMCELL system. The successful isolation and purification of hepatocytes are crucial for various applications in regenerative medicine, drug development, and disease modeling. Our findings shed light on which MACS approach may yield the most functionally active hepatocyte organoids, providing valuable insights for researchers and clinicians working in this field.

Our results demonstrated that the Miltenyi MACS approach outperformed the STEMCELL method in terms of hepatocyte enrichment and functionality. This conclusion is supported by several key observations in our experiments including increased human albumin levels and retained CK18 expression. The enhanced albumin production suggests that the Miltenyi approach is more efficient in isolating functional hepatocytes (Figure 4.2B), which is crucial for *in vitro* and *in vivo* application CK18 is a specific marker for hepatocytes, immunostaining techniques were used to assess the presence of CK18 in the sorted organoids. Our results (Figure 4.2C)

demonstrated that Miltenyi MACS sorted organoids maintained a higher level of CK18 expression compared to those sorted with the STEMCELL method. This finding reinforces the notion that the Miltenyi approach is superior in retaining hepatocyte-specific markers, which is vital for ensuring the identity and functionality of the isolated cells. The column-based Miltenyi system allows for a more precise separation of hepatocytes from other cell types in the organoids, minimizing the risk of cross-contamination and ensuring a higher degree of purity. This level of purity is crucial, especially in applications where hepatocyte function is of utmost importance. Having discussed the superior performance of the Miltenyi MACS system in hepatocyte organoid purification, we now turn our attention to the critical aspect of dissociation techniques, which play a pivotal role in the separation method efficacy.

The implementation of various cell dissociation solutions, including TrypLE and Cell Recovery Solution, allowed us to evaluate their efficiency in achieving this separation. The results indicated that using a combination of Cell Recovery Solution and TrypLE, along with magnetic labeling yielded the most promising outcomes. This approach not only achieved a greater degree of cholangiocyte elimination but also improved cell viability. These findings are crucial in the context of hepatocyte culture, as purity and viability are fundamental for the successful long-term maintenance of hepatocyte function.

The study also delved into the challenge of maintaining hepatocyte functionality over extended periods. The initial experiment involved a 42-day culture period, where organoids were subjected to regular passaging and replating every 14 days. As anticipated, we observed a decrease in albumin levels over this extended timeframe, which can be attributed to the longevity of cells in culture as well as the repeated process of passaging cells every 2 weeks. This highlights the

limitations of standard culture practices in sustaining hepatocyte function over the long term.

In response to this decline, we introduced Magnetic-Activated Cell Sorting (MACS) as a potential solution. We have seen the utilization of MACS in high throughput sorting of target cells based on surface markers allowing for the capability to sort specific biological targets from complex mixtures with high purity and recovery(58,59). Two different approaches were explored: passage and sorting every two weeks and sorting and splitting every 7 days for the initial 14 days. The data revealed a significant decrease in human albumin levels when organoids underwent passage and sorting every two weeks. This decline could be attributed to the removal of essential cells that are necessary for maintaining hepatocyte functionality. However, when we employed the 7-day sorting and splitting method for the initial 14 days, there was still a decrease in albumin production, but it was less pronounced compared to the control group.

The findings from this study have several important implications for the field of hepatocyte culture and regenerative medicine. First and foremost, effective separation techniques, such as the combination of Cell Recovery Solution and TrypLE, can significantly improve the purity and viability of hepatocyte cultures, which is essential for the reliable assessment of hepatocyte function and drug metabolism.

Secondly, the study underscores the challenges associated with long-term hepatocyte culture. It highlights the importance of optimizing culture conditions, including the timing of passage and sorting, to maintain hepatocyte function over extended periods. Although the 7-day sorting and splitting method showed some promise in mitigating the decline in albumin levels, it also revealed the complexity of balancing cell preservation with continuous organoid growth.

In conclusion, the results of this study provide valuable insights into the purification and maintenance of adult human hepatocyte organoids. These findings can inform future research aimed at optimizing hepatocyte culture systems and furthering our understanding of liver regeneration and disease modeling in vivo (60), with the goal of advancing therapeutic approaches for liver-related pathologies.

In summary, MACS significantly contributes to the long-term functionality of hepatocyte organoids by enabling the isolation and purification of hepatocyte populations. Maintaining the functionality of these organoids over extended periods is crucial for their applications in liver disease modeling, drug testing, and regenerative medicine. Ongoing efforts focus on refining culture conditions and differentiation protocols to enhance the longevity of hepatocyte organoids and their relevance in various liver research and therapeutic applications.

4.4 METHODS

4.4.1 *Organoid culture of hepatocytes*

Cryopreserved hepatocytes were thawed into 37°C medium and quickly spun down at 70 x g. Cells were mixed with 45% organoid media and 55% Matrigel and seeded in 20 µl droplets in each well of 48-well plates. After Matrigel had solidified, 200 µl of organoid medium was added to each well. Organoid medium: 40% Basal medium (DMEM/F12, 1x GlutaMAX, 1x HEPES, 1x penicillin-streptomycin, 2% B27, 10 mM nicotinamide, 1.25 mM N-acetyl cysteine, 10 nM gastrin), 50% Wnt3a conditioned medium, 10% Rspo1 conditioned medium, 50 ng/ml EGF, 5 µM A83-01, and 10 µM y-27632. Medium was refreshed every 2-3 days with care not to disturb the Matrigel droplet. Organoid size and growth were quantified from minimum intensity projections of brightfield z-stacks taken on a Nikon Eclipse Ti inverted high-resolution widefield microscope.

4.4.2 *Splitting hepatocyte organoids*

Organoids were harvested from Matrigel, using either Cell Recovery Solution (Corning) or TrypLE (Thermo) or a combination of both, for 30 minutes and 10 minutes, respectively. Cells are spun down at 70x g and mixed with 45% organoid media and 55% Matrigel and seeded in 20 µl droplets in each well of 48-well plates. After Matrigel had solidified, 200 µl of organoid medium was added to each well. Medium was refreshed every 2-3 days with care not to disturb the Matrigel droplet. Organoid size and growth were quantified from minimum intensity projections of brightfield z-stacks taken on a Nikon Eclipse Ti inverted high-resolution widefield microscope.

4.4.3 *Brightfield microscopy and morphometric analysis*

Brightfield z-stack images were taken in the center of each organoid well at multiple timepoints on a Nikon Eclipse Ti inverted high-resolution widefield microscope. Z-stacks were flattened into a single image using a minimum intensity projection (MinIP) with FIJI or Nikon NIS-Elements software. Organoid size and growth were quantified from MinIP images in ImageJ software and graphed with GraphPad Prism software.

4.4.4 *Albumin ELISA*

Organoid media was collected every 2-3 days and frozen. Secreted human albumin was then measured in media via enzyme linked immunosorbent assay (ELISA) using a goat anti-human albumin coating antibody and horseradish peroxidase-conjugated goat anti-human albumin detection antibody (Bethyl E80-129).

4.4.5 *Statistical Analysis*

Data in graphs are expressed as the mean ± SEM, as denoted in figure legends. Statistical significance was determined with PRISM software using t-test, one-way ANOVA, or two-way ANOVA followed by Sidak's, Dunnett's, or Tukey's multiple comparison test, as denoted in figure legends.

Chapter 5. Therapeutic potential of human hepatocyte organoids in an immunodeficient mouse model of hereditary tyrosinemia type I

5.1 INTRODUCTION

To investigate therapeutic potential of human hepatocyte organoids in liver diseases, our first approach was to test whether human hepatocyte organoids can be engrafted into an immunodeficient mouse model of hereditary tyrosinemia type I. This investigation offers a unique opportunity to explore the complexities of hepatocyte organoid behavior and their application in inducing humanization within murine hosts.

At the center of this study are Fah−/−, Rag2−/−, and Il2rg−/− (FNRG) mice, a well-established immunodeficient model for studying human cell engraftment with human hepatocyte organoids and a model of hereditary tyrosinemia type I due to the deficiency in the enzyme fumarylacetoacetate hydrolase (FAH) which is the last enzyme in the tyrosine catabolic pathway (61). Immunodeficient mice are created through specific genetic modifications, including the introduction of three key mutations: Fah^-/-, Rag2^-/-, and Il2rg^-/-. The Fah^-/- mutation disrupts the fumarylacetoacetate hydrolase (FAH) gene, inducing a metabolic defect in these mice, which acts as a safeguard and enables the control of their health using the drug 2-(2-nitro-4-(trifluoromethyl) benzoyl) cyclohexane-1,3-dione (NTBC) (55,62). Failure to administer NTBC can lead to the development of liver disease in these mice (55,63–65). NTBC cycling can lead to expansion of xenograft hepatocytes in FNRG. The specific cues triggering this expansion process remain unidentified; however, it is postulated that this method operates by providing signals originating from the injured mouse liver and by creating available space as murine hepatocytes die

(1). The Rag2^-/- mutation signifies the absence of the Rag2 gene, crucial for B and T lymphocyte development, rendering Rag2^-/- mice functional B and T lymphocytes (66). The Il2rg^-/- mutation also disrupts the Il2rg gene, which encodes the common gamma chain of cytokine receptors, resulting in impaired natural killer (NK) cell function (67). Therefore, FNRG mice exhibit deficiencies in T and B cells and impaired NK cell function, further contributing to their immunodeficiency (3). Utilizing FNRG mice, we have leveraged this model by utilizing multiple lots of human hepatocytes and growing them into organoids, providing a valuable method for testing the organoid therapeutic potential in this disease model.

We grew hepatocyte organoids over a 14-day in vitro period, followed by their introduction into the FNRG mice via intrasplenic injection. This method enables the uniform distribution of organoids, which travel through the spleen to reach the liver. However, intrasplenic injections are limited by lower number of cells that can be injected compared to the engineered liver tissue seeds approach. Engineered liver tissues seeds offer the advantage of allowing approximately three times more cells to be implanted in the mice compared to intrasplenic injections.

This process sets the stage for a comprehensive examination of hepatocyte behavior and function, bringing into focus the roles of specific markers such as cytokeratin 18 (CK18), E-cadherin (ECAD), and cytokeratin 19 (CK19) (68–70). Our findings provide evidence of organoid functionality and prompt us to consider the prospect of their therapeutic application. As we progress further into the study, we look at the differences that emerge between the cryopreserved and organoid groups. This phase of our research unravels unexpected events. It sheds light on the complex challenges associated with long-term maintenance and expansion of human hepatocytes within the murine hosts. It details the intricate world of human hepatocyte organoids and their

interaction with immunodeficient mice. Adult human hepatocyte organoids can engraft and be passaged, as seen with mouse-passaged primary human hepatocytes (mpPHHs) and humanize FRNG mice.

5.2 RESULTS

In our study, we employed FNRG mice to investigate the potential of engraftment and passaging of hepatocyte organoids in the context of liver injury. To assess this potential, we initiated our experiments with human hepatocytes derived from two distinct sources: lot #4143 and lot #8375, our standard donor, as described in Chapter 3. These hepatocytes were cultured as organoids for 14 days in vitro before being dissociated and utilized for intrasplenic injection into the FNRG mice. For comparison, we also included a control group of freshly thawed cryopreserved human hepatocytes.

Immunofluorescence staining (Figure 5.1B) and subsequent quantitative analyses (Figure 5.1D) revealed a substantial proportion of hepatocytes exhibiting a positive expression of cytokeratin 18 (CK18) and E-cadherin (ECAD). In contrast, the percentage of cells expressing cytokeratin 19 (CK19) was notably lower. Both lot 8375 and lot 4143 successfully underwent engraftment and exhibited a progressive increase in albumin production over time. Notably, lot 8375 displayed increased albumin levels when compared to lot 4143. This observation could potentially be associated with the heightened presence of CK18-positive organoids at the 14-day mark, suggesting a correlation between CK18 expression and albumin production. These cells were then introduced into the FNRG mice via intrasplenic injection to determine whether the organoids could induce humanization within the murine hosts.

Throughout our study, we monitored human albumin levels (Figure 5.1C-D) and observed differences between the cryopreserved and organoid groups. Encouragingly, our findings indicated that the organoids exhibited a similar functional capacity to the cryopreserved human hepatocytes, providing compelling evidence that the organoids indeed grafted and expanded within the livers

in the FNRG mice to a comparable level as the freshly thawed human hepatocytes.

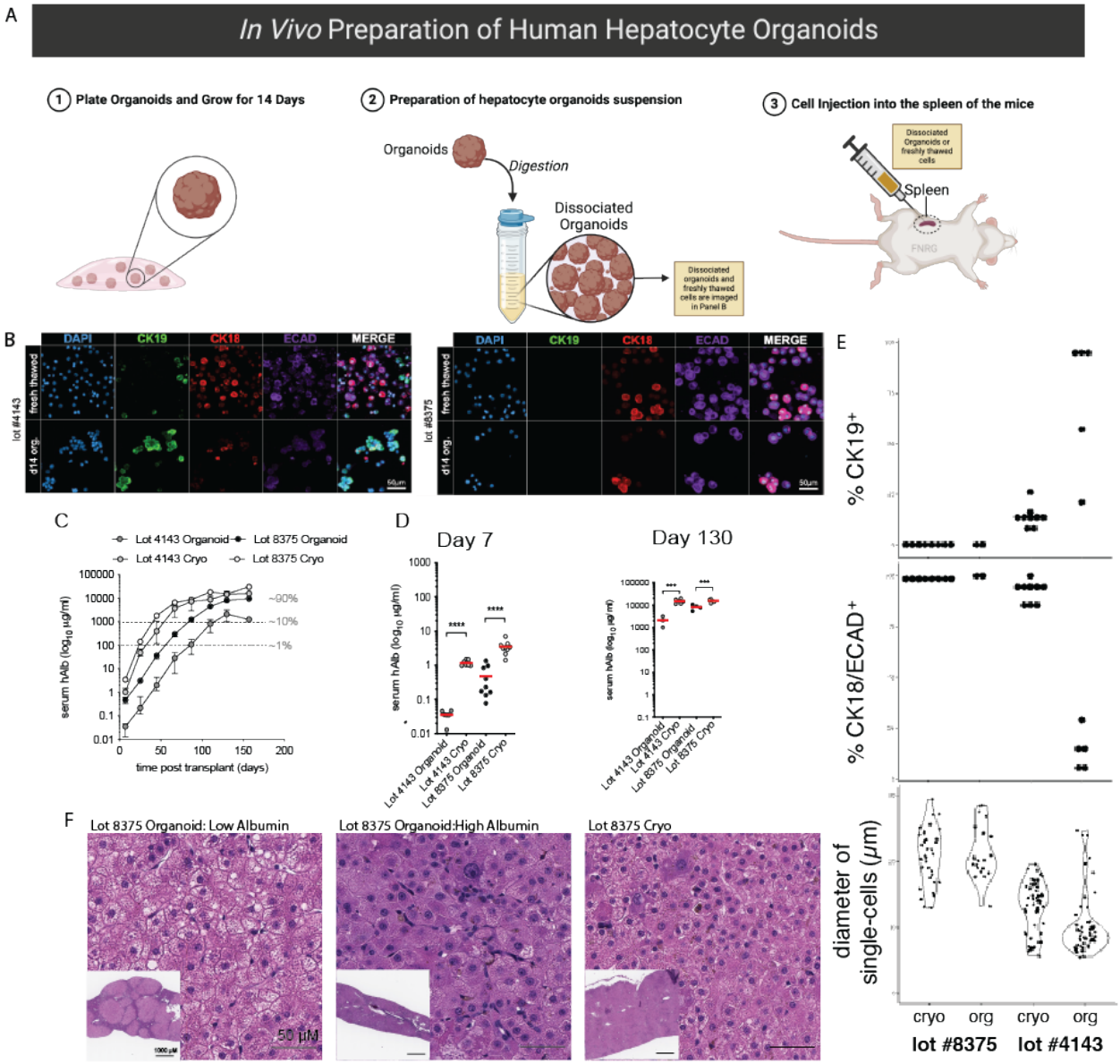

Figure 5.1: Repopulation of FNRG Mice livers using Adult Human Hepatocyte Organoids

(A) Experimental schematic of the *in vivo* preparation of human hepatocyte organoids for intrasplenic injection.

(B) Immunofluorescence images comparing freshly thawed cryovial cells with Day 14 human hepatocyte organoids from two separate lots (lot #4143 and lot #8375) stained for CK18 (red), CK19 (green), Epithelial cadherin (purple), and Hoechst (blue). Scale bar = 50 µm.

(C) Albumin secretion measured by human albumin ELISA in FNRG mice at Day 7 and Day 130

comparing transplanted freshly thawed cryovial cells with human hepatocyte organoids from two separate lots (lot #4143 and lot #8375)

(D) Albumin secretion measured by human albumin ELISA in FNRG mice with 130 days comparing transplanted freshly thawed cryovial cells with human hepatocyte organoids from two separate lots (lot #4143 and lot #8375)

(E) Quantifications of immunofluorescence images, including Percentage of CK19 (top), Percentage of CK18/ECAD (middle), and the diameter of single cells (bottom) comparing transplanted freshly thawed cryovial cells with human hepatocyte organoids from two separate lots (lot #4143 and lot #8375)

(F) Representative histochemical images representing H&E-stained liver graft sections with injected organoids at varying albumin production levels and freshly thawed cryovial cells. Low magnification scale bar = 1000μm and high magnification scale bar = 50μm

To investigate deeper, following our observation of successful humanization induced by the organoids in the FNRG mice, we proceeded to passage both the cryopreserved and organoid groups sourced from our standard donor, lot #8375. Over a 150-day duration, we monitored the levels of human albumin (Figure 5.2A-B). A marked disparity between the two groups became apparent during this time frame.

Between Days 50 and 100, a significant event unfolded: a notable reduction in the number of mice was observed in both groups. Furthermore, the remaining mice demonstrated a limited ability to achieve a level of humanization exceeding 10%. This outcome underscores a pivotal aspect of our study, emphasizing the complexities and constraints associated with the limitation of extended-term maintenance and expansion of human hepatocyte organoids within the mice.

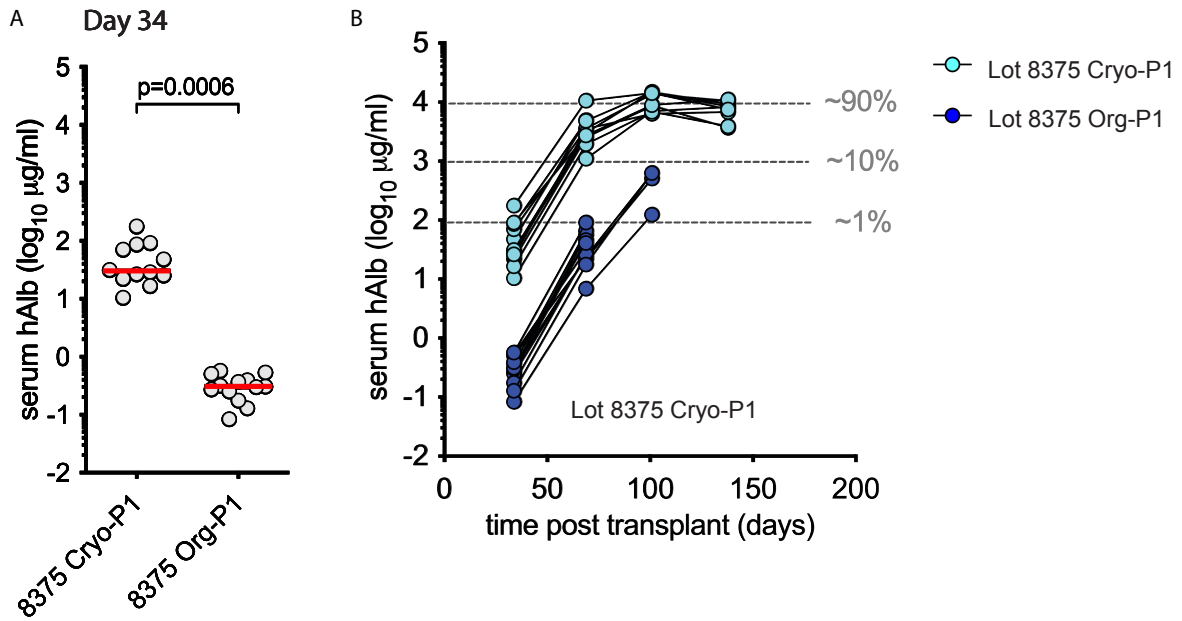

Figure 5.2: Downstream Passaging Expansion of Organoids in Humanized FNRG Mice

(A) Albumin secretion measured by human albumin ELISA in FNRG mice at Day 34 comparing Passaged Cryovial Human hepatocytes with Passaged Adult Human Hepatocyte Organoids.

(B) Albumin secretion measured by human albumin ELISA in FNRG mice within 150 days post-transplant.

In conjunction with the transplantation of the passaged organoids, a survival study was conducted to assess and compare the outcome between the lot 8375 organoid-injected mice and a control group (Sham mice), which received an injection of Hank's Balanced Salt Solution (HBSS). As part of this assessment, we quantified human albumin levels (Figure 5.3A) and observed a promising increase in the measurements. However, it is worth noting that the mortality of all mice in both groups occurred before a subsequent measurement could be obtained, as evidenced by the survival curve (Figure 5.3B). Within the framework of this chronic liver injury model, our analysis did not reveal a statistically significant difference in the observed outcomes between the two experimental groups.

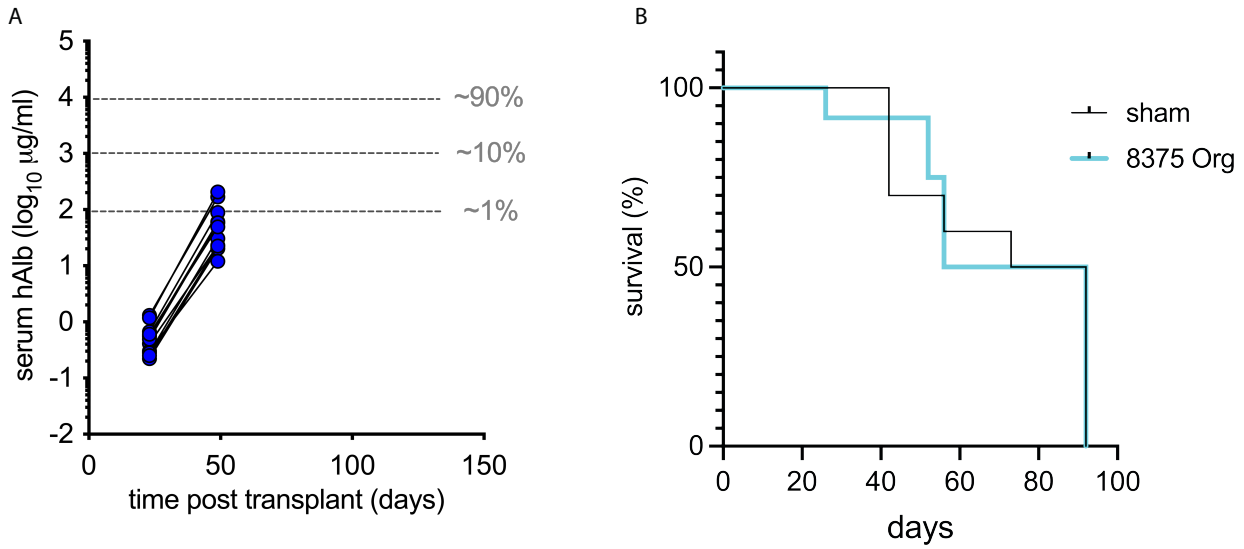

Figure 5.3: Survival Study Utilizing the FNRG Mouse Model of Chronic Liver Injury with Adult Human Hepatocyte Organoids

(A) Albumin secretion measured by human albumin ELISA in FNRG mice.

(B) Survival Curve of Organoid transplanted and Sham FNRG mice.

5.3 DISCUSSION

Our study commenced using two distinct sources of human hepatocytes, lot #4143 and our standard donor, lot #8375, which were cultured as organoids and injected intrasplenically into FNRG mice. We also included a control group with freshly thawed cryopreserved human hepatocytes. Immunofluorescence staining demonstrated positive expression of CK18 and ECAD in a substantial proportion of hepatocytes from the organoid groups, while CK19 expression was notably lower. This observation suggested that hepatocyte organoids had the potential for engraftment in the FNRG mice and further supported their structural integrity. Human albumin levels were monitored, and it indicated that the organoids exhibited functional capacity similar to cryopreserved human hepatocytes, providing a therapeutic potential for tyrosinemia and compelling evidence of their ability to induce humanization in the FNRG mice.

Subsequently, we conducted a more profound investigation by passaging both the cryopreserved and organoid groups sourced from lot #8375. Over a 150-day duration, human albumin levels were monitored. An intriguing finding emerged as a marked disparity between the two groups became apparent. Between Days 50 and 100, a significant reduction in the number of mice was observed in both groups, and the mice that remained displayed a limited ability to achieve a level of humanization exceeding 10%. This marked difference indicates that further optimization, such as better dissociation of cells from organoids after culture, is necessary for proper grafting and expansion of human hepatocyte organoids within the murine hosts.

In conjunction with the transplantation of the passaged organoids, we conducted a survival study to investigate the impact. Specifically, we compared the survival rates between a group of mice that received the 8375 lot of organoids via injection and a control group, consisting of "Sham mice," which received an injection of HBSS. During this study, we implemented a regimen involving the administration of NTBC (2-(2-nitro-4-trifluoromethylbenzoyl) cyclohexane-1,3-dione) at intervals of 2-3 weeks following organoid transplantation.

While we measured human albumin levels in the mice and observed a promising increase in these measurements, it is crucial to acknowledge that all mice in both groups succumbed to mortality before subsequent measurements could be recorded. This mortality trend became apparent in the survival curve, coinciding with the periods when NTBC was temporarily discontinued.

Within the context of our chronic liver injury model, our analysis did not reveal any statistically significant disparities in the observed outcomes between the two experimental groups. With this model, the cycling of NTBC appears to be a critical factor. However, it is challenging to

definitively assert that the pause of NTBC administration is the sole contributor to the observed mortality. The organoid group of mice experienced mortality before attaining 10% engraftment, presumably due to constraints inherent to organoid culture. This phenomenon may be attributed to the substantial proliferation of hepatocytes before their introduction into the FNRG murine models. This issue could be mitigated in future investigations by implementing telomere length analysis.

Our studies offer valuable insights into the potential of hepatocyte organoids for engraftment and their functional capacity in an FNRG mouse model of liver injury. The lack of statistically significant differences in outcomes between the organoid-injected mice and the control group in our chronic liver injury model indicates the need for further research and optimization of the experimental approach. Future studies should focus on refining the protocols for organoid transplantation and exploring potential strategies to enhance the survival and function of transplanted hepatocytes.

In conclusion, our study contributes to understanding the engraftment and functional capacity of hepatocyte organoids in a murine model of liver injury. It highlights the complexities and challenges associated with the long-term maintenance and expansion of human hepatocytes within a murine host. It highlights the need for further investigations to optimize this approach for potential clinical applications.

5.4 METHODS

5.4.1 *Organoid culture of hepatocytes*

Cryopreserved hepatocytes were thawed into 37°C medium and quickly spun down at 70 x g. Cells were mixed with 45% organoid media and 55% Matrigel and seeded in 20 µl droplets in each well of 48-well plates. After Matrigel had solidified, 200 µl of organoid medium was added to each well. Organoid medium: 40% Basal medium (DMEM/F12, 1x GlutaMAX, 1x HEPES, 1x penicillin-streptomycin, 2% B27, 10 mM nicotinamide, 1.25 mM N-acetyl cysteine, 10 nM gastrin), 50% Wnt3a conditioned medium, 10% Rspo1 conditioned medium, 50 ng/ml EGF, 5 µM A83-01, and 10 µM y-27632. Medium was refreshed every 2-3 days with care not to disturb the Matrigel droplet. Organoid size and growth were quantified from minimum intensity projections of brightfield z-stacks taken on a Nikon Eclipse Ti inverted high-resolution widefield microscope. Organoids were grown for 14 days.

5.4.2 *Organoid Dissociation*

Organoid fragments were prepared following 30 minutes of digestion in Cell Recovery solution on ice. After organoid digestion from Matrigel, cells are spun down at 70 x g. Organoids are resuspended in TrypLE and incubated for 5 minutes, strained with 70 µm cell strainer. Wash cell strainer with HBSS, 0.0025 mg/ml DNase I, 2% FBS (HBSS-DF) and rinse with HBSS, dropwise. Sediment cells at 70 x g for 5 minutes and resuspend in HBSS, followed by mechanical dissociation for hemocytometer quantification.

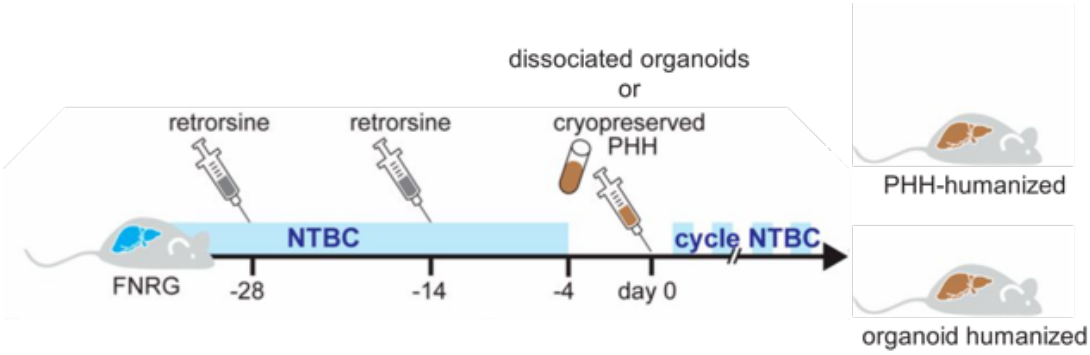

Figure 5.4: Experimental schematic of FNRG mice treated with retrorsine 4 and 2 weeks prior to transplantation with cryopreserved PHHs or dissociated organoids and NTBC cycling

5.4.3 *Implantation and induction of liver injury*

All surgical procedures were conducted according to protocols approved by Rockefeller University Institutional Review Board. 6-week-old female (Fah−/−), Rag2−/− and Il2rg−/− (FNRG) where FNRG mice were maintained on an ad libitum chow diet with amoxicillin and drinking water containing 16 mg/mL NTBC (Yecuris). Mice were housed under a 12-h light cycle from 7:00 AM (ZT0) to 7:00 PM (ZT12). Retrorsine (catalog no. R0382; Sigma Aldrich) was dissolved at 20 mg/mL in 100% ethanol at 56 °C and stored in aliquots at −20 °C, retrorsine was administered at 2-wk intervals, typically the first dose at 3 to 4 weeks prior to transplantation and a second dose 2 to 3 weeks prior to transplantation (Figure 5.4). Female FNRG recipients were withdrawn from NTBC 4 to 5 days prior to surgery. Briefly, under sterile conditions and using isoflurane anesthesia, the skin was cleaned with povidone iodine, and a 0.5- to 1-cm incision was created over the left flank, after which the peritoneum was mobilized and opened. The ventral tip of the spleen was mobilized onto the peritoneum, and 65 µL of cell suspension of 0.5 million cells were injected into the spleen using a 28-gauge insulin syringe. After hemostasis was achieved by applying pressure to the injection site, the peritoneum was closed using 4.0 Vicryl suture (Ethicon) and the skin was closed using metal Mikron Autoclips (BD Biosciences). Mice received two doses of postoperative buprenorphine (Abbot

Animal Health) 0.05 mg/kg for analgesia. Metal clips were removed 14 days after surgery.

5.4.4 *Histochemical staining, immunofluorescent staining, and microscopy*

Immunofluorescence staining of organoids was performed by deparaffinizing sections, performing antigen retrieval, blocking with normal donkey serum for 1 hour at room temperature, then incubating with primary antibody overnight at 4°C. The following day, sections were washed with PBS-T and then incubated with secondary antibody + Hoechst 33342 (Thermo H3570) for 1 hour at room temperature, washed, and mounted with Fluoromount-G (Invitrogen). All antibody information is included in Table 1. Images were obtained using a Nikon Eclipse Ti inverted high-resolution widefield microscope or a Nikon A1R scanning confocal microscope. Images were processed using Adobe Photoshop or ImageJ software. For morphometric analyses, images were thresholded, and pixels were measured using ImageJ software.

5.4.5 *Albumin ELISA*

Serum was obtained from tail veins or retroorbital plexus. Culture supernatants were obtained at indicated time points. Human Albumin was quantified using sandwich ELISA methods (Bethyl Labs).

5.4.6 *Statistics*

Groups were compared by the Student t-test. Correlations were calculated using the Spearman correlation coefficient. All statistical analyses were done using Prism 8 software (Graphpad). This test was used to determine if there is a significant difference between the mean of two independent groups.

Chapter 6. Assess Therapeutic Efficacy of Adult Human Hepatocyte Organoids using Acetaminophen (APAP) Induced Liver Injury Model

6.1 INTRODUCTION

Drug-Induced Liver Injury (DILI) is a frequently encountered condition resulting from the consumption of commonly used medications in quantities that are detrimental to the human body. Acetaminophen (APAP), a widely utilized non-prescription analgesic and antipyretic drug, holds a prominent position in this category and accounts for approximately 50% of all instances of Acute Liver Failure (ALF), with a substantial 30% mortality rate (71).

While within therapeutic dosage ranges, APAP is generally considered safe; exceeding these limits can lead to severe liver toxicity and, in extreme cases, fatality (71) The over-metabolism of APAP depletes intracellular glutathione and escalates the levels of N-acetyl-p-benzoquinoneimide (NAPQI). This, in turn, triggers oxidative stress, DNA damage, and the necrosis of hepatic cells, resulting in liver damage. Acetaminophen overdose is identified as one of the primary causes of ALF in the United States (71). In severe instances, liver transplantation remains the only viable option to potentially save the patient's life. Therefore, APAP-induced liver injury is becoming an increasingly significant public health concern (67).

As an emerging approach, human hepatocyte organoids are being explored as an alternative method for the treatment of APAP-induced liver injury. This chapter centers on the xenograft implantation of human hepatocyte organoids in APAP-induced ALF model in immune deficient NOD-SCID IL2Rγ^null (NSG) mice, emphasizing the therapeutic potential of hepatocyte

organoids in ALF models.

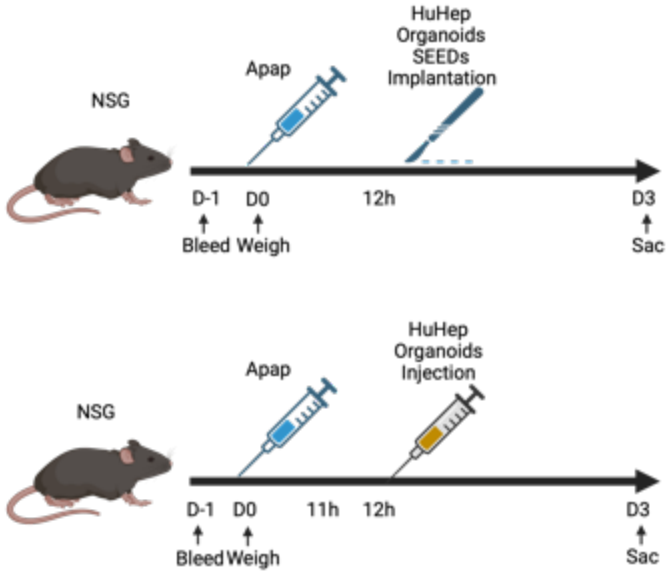

Figure 6.1: Schematic of Approaches for APAP-Induced Liver Injury Model in NOD-SCID IL2Rγ^null (NSG) Mice Utilizing Engineered Liver Tissue Seeds and Intrasplenic Injections

6.2 RESULTS

We chose to examine two approaches – 1) engineered liver tissue seeds encapsulated with fibrin and implanted into perigonadal fat pads and 2) injection of organoids directly into perigonadal fat pads to analyze the APAP induced liver injury model.

6.2.1 *Perigonadal Fat Pad Injection*

We employed an alternative approach involving the perigonadal fat pads of NSG mice for the injection of the adult human hepatocyte organoids. This method allowed us to measure therapeutic recovery, utilizing the same parameters as the APAP-induced liver injury model using engineered liver tissue seeds, which are adult human hepatocyte organoids grown *in vitro* dissociated from Matrigel and encapsulated with fibrin hydrogel to be implanted *in vivo*.

To evaluate the recovery within the context of the Drug-Induced Liver Injury (DILI) model, we monitored two critical parameters: body weight and body scores. Body scores, behavioral assessments including levels of activity; grooming, eating, drinking, and overall mobility; were specifically recorded to gauge the condition of the mice, and these assessments revealed differences between the organoid-treated group and the HBSS-injected control group. The body scores (Figure 6.2A), exhibited variations between the organoid-treated and control groups. Notably, the organoid group displayed more favorable body scores, indicative of a better overall condition when compared to the HBSS-injected control group.

Upon completion of the 5-day *in vivo* experimental period, we conducted tests to measure the levels of alanine transaminase (ALT) and aspartate aminotransferase (AST) enzymes in the collected blood, as these enzymes are primarily found in the liver and can indicate liver damage or disease. The ratio of AST to ALT (Figure 6.2B), showing comparable results between the organoid and control groups, suggesting similar extents of liver injury. In a healthy liver, ALT levels are typically higher than AST levels, resulting in a low AST/ALT ratio. When liver cells are damaged, ALT is released into the bloodstream in greater quantities than AST, causing an increase in the ALT level and a decrease in the AST/ALT ratio. This pattern is often seen in cases of acute liver injury (70). Furthermore, we conducted human albumin testing (Figure 6.2C), notably, the organoid group exhibited significantly higher human albumin levels compared to the sham group, indicating a more robust recovery response. However, these levels did not surpass those observed in the no APAP group, underscoring the influence of the absence of APAP on the overall recovery response.

Our experimental approach, which involved the use of the adult human hepatocyte organoids in the perigonadal fat pad of NSG mice, demonstrated improved recovery as evidenced by body scores and human albumin levels when compared to the control group. These results underscore the potential therapeutic benefits of our approach in mitigating drug-induced liver injury, with some variability observed in comparison to the No APAP group.

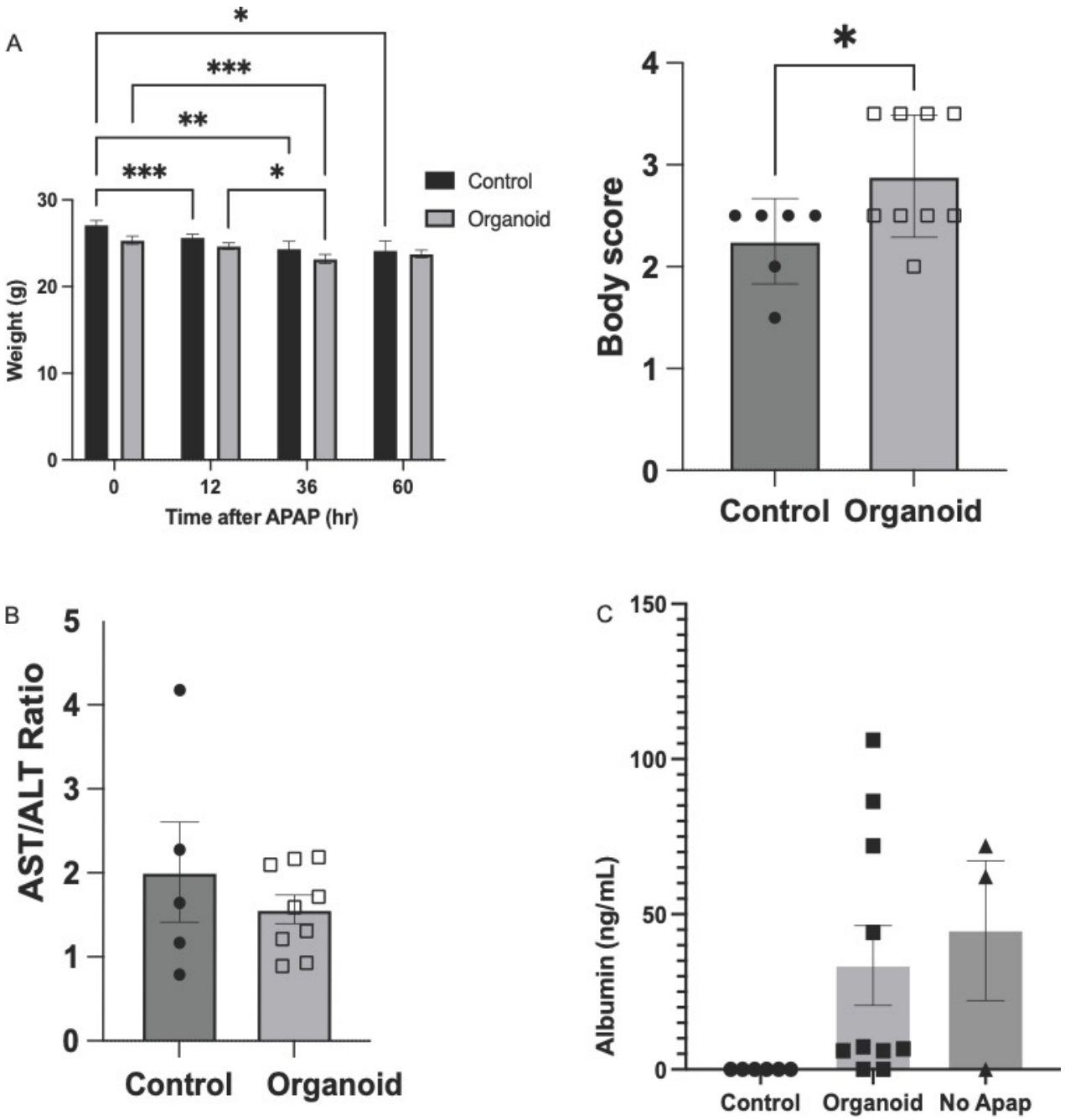

Figure 6.2: Investigation of Therapeutic Effects and Engraftment Potential of Organoids in APAP-Induced Liver Injury Model in NSG Mice using Perigonadal Fat Pad Injection

(A) Relationship between body weight and body score in NSG Mice

(B) AST and ALT ratio measured in mouse blood. Data represented as mean +/- SEM of the control and organoid groups at Day 5

(C) Secreted human albumin measured in mouse blood by human albumin ELISA. Data represented as mean +/- SEM of the control and organoid, and No APAP groups after 5 days.

6.2.2 *Engineered liver tissue seeds*

To examine whether the engineered liver tissue seeds ameliorates APAP induced ALF, we implanted engineered liver tissue seeds with adult human hepatocyte organoids into NSG mice after 12 hours of APAP injection and compared their responses to a control group given sham seeds made without organoids.

To analyze the engraftment potential of hepatocytes grown as organoids in engineered tissue seeds, we cultured adult human hepatocytes for seven days and encapsulated them within fibrin hydrogels, creating engineered liver tissue seeds and then implanted into the perigonadal fat pad of NSG (NOD-SCID IL2Rγ^null) mice, which are immunocompromised and lack mature T, B, and functional NK cells and thus can receive xenograft implants. To access, the recovery of the Drug-Induced Liver Injury (DILI) model, two key parameters were measured: body weight and body score (Figure 6.3A). Body weight was monitored every 24 hour over a 60-hour period, while body scores were recorded at 36 hours, a time point when the NSG mice were experiencing the peak of their distress. Figure 6.3A illustrates the changes in body weight over the 60-hour observation period. Notably, a significant difference in the body score at 36 hours was observed between the sham group and the group treated with human hepatocyte organoids. In general, the organoid-treated mice displayed a better overall condition, as reflected by their weight and body score trends.

Serum samples were collected at the conclusion of the 3-day experimental period. We measured two key liver injury markers, Aspartate Aminotransferase (AST) and Alanine Aminotransferase (ALT) and plotted their ratio (Figure 6.3B). Remarkably, no significant differences were observed in the AST/ALT ratio between the sham and organoid groups, possibly indicating a similar extent

of liver injury in both groups.

Conversely, we also conducted human albumin testing and found a notable difference among the groups. Figure 6.3C depicts the human albumin levels in the sham, no APAP, and organoid groups. Significantly higher levels of human albumin were detected in the organoid-treated mice compared to the sham group, indicating a robust grafting of the liver seeds in the organoid group which did not get reduced in the groups injured by APAP.

Our findings demonstrate that the use of adult human hepatocyte organoids integrated into engineered liver tissue seeds in the NSG mouse model leads to improved recovery in terms of body score and human albumin levels. These results indicate the potential therapeutic efficacy of this approach in mitigating drug-induced liver injury.

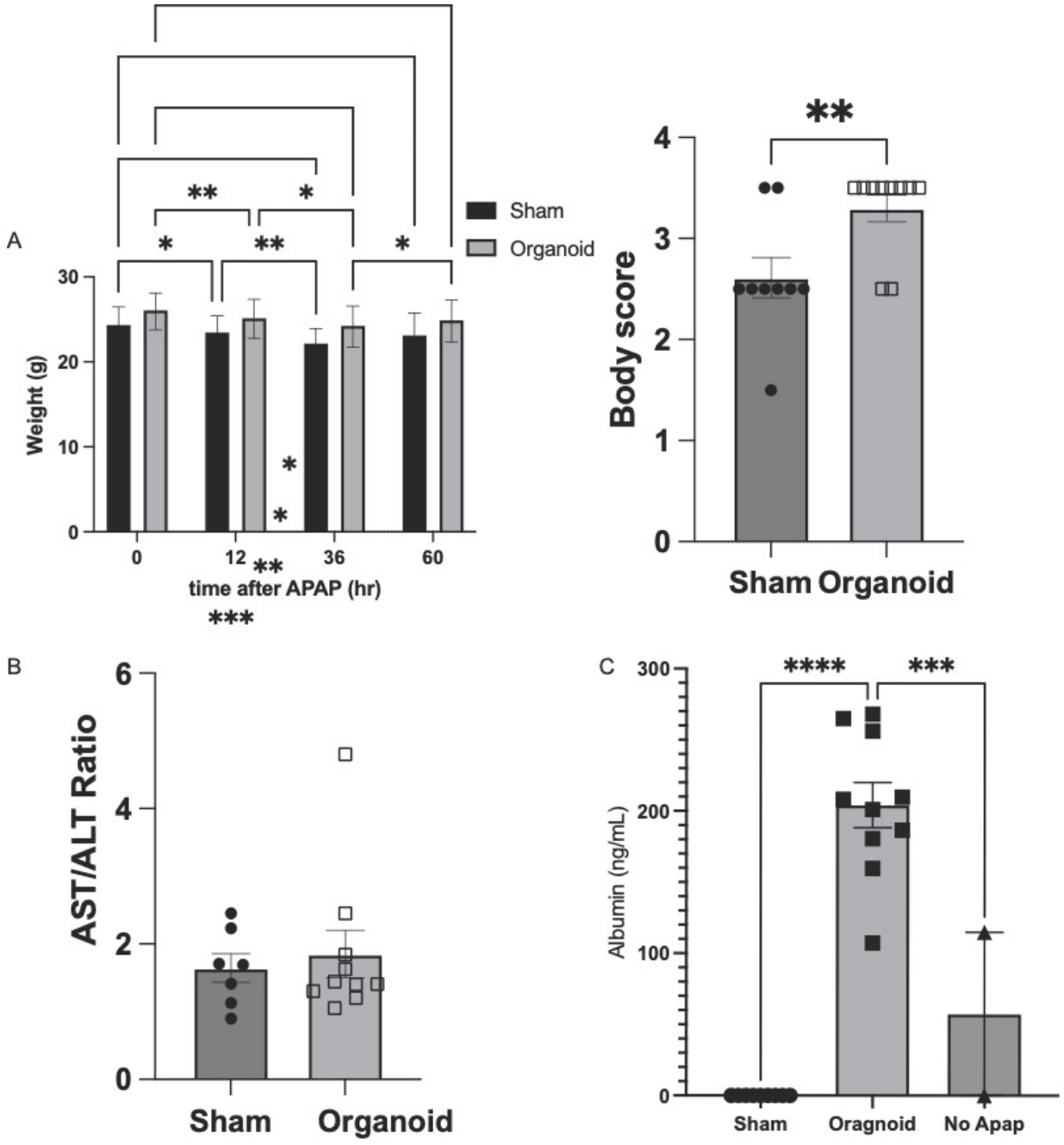

Figure 6.3: Investigation of Therapeutic Effects and Engraftment Potential of Organoids in APAP-Induced Liver Injury Model in NSG Mice using Engineered liver tissue seeds.

(A) Relationship between body weight and body score in NSG Mice

(B) AST and ALT ratio measured in mouse blood. Data represented as mean +/- SEM of the sham and organoid groups at Day 5

(C) Secreted human albumin measured in mouse blood by human albumin ELISA. Data represented as mean +/- SEM of the sham and organoid, and No APAP groups after 5 days.

To expand our knowledge on the effects of APAP in a NSG DILI mouse model, further experiments were conducted, altering experimental factors, we conducted additional experiments, varying experimental conditions such as incorporating fasting periods and adjusting the initial concentration of APAP administered. Specifically, we administered 500 mg/kg of APAP, preceded by a 12-hour fasting period, 12 hours prior to surgical intervention (Figure 6.4A). We implanted engineered liver tissue seeds containing adult human hepatocyte organoids into NSG mice and monitored their response.

To assess the recovery in our DILI model, we measured two key parameters: body weight and body score (Figure 6.4B). Body weight was monitored every 24 hours over a 60-hour period, while body scores were noted at 36 hours, a time point when the NSG mice were experiencing the peak of their distress. No significant differences were observed between the sham group and the group receiving engineered liver tissue seeds with adult human hepatocyte organoids. Similarly, there were no significant variations in body scores at 36 hours between the sham group and the group treated with human hepatocyte organoids. Despite promising outcomes in prior experiments, this study did not yield statistically significant results despite an increased sample size. Overall, mice treated with organoids did not exhibit noteworthy differences in weight and body scores compared to controls.

Though no significant data was obtained, serum samples were collected at the conclusion of the 3-day experimental period. We assessed two key liver injury markers, AST and ALT and plotted their ratio (Figure 6.4C), no significant differences were observed in the AST/ALT ratio between the sham and organoid groups. Similar to previous experiments, this lack of difference may indicate a comparable extent of liver injury in both groups.

In contrast, human albumin testing revealed a notable disparity among the groups. Figure 6.4D illustrates the human albumin levels in the sham, no APAP, and organoid groups. Significantly higher levels of human albumin were detected in the organoid-treated mice compared to the sham group, indicating a robust grafting of the liver seeds in the organoid group which did not get reduced in the groups injured by APAP. Figure 6.4E depicts the survival curve of the NSG mice transplanted with organoids versus sham controls.

Conclusively, our findings from this experiment lack statistically significance to support the potential therapeutic efficacy of this approach in mitigating drug-induced liver injury. Instead, we observed a decline in animal survival, which we attribute to the combined the combined effects of adding a fasting period and the concentration of APAP administration.

Building upon the outcomes of prior experiments, we inferred that the combined impact of the 12-hour fasting period and the APAP dosage led to excessive liver injury, impeding recovery in mice treated with engineered liver tissue seeds containing organoids. To expand on this observation, we reduced the APAP dose from 500 mg/kg to 400mg/kg while retaining the 12-hour fasting period before implantation (Figure 6.5A). Nonetheless, no significant data was garnered from assessments of body weight and body score. Intriguingly, a higher body score was noted in NSG mice that did not receive APAP (Figure 6.5B). Evaluation of AST/ALT ratios and albumin levels (Figure 6.5C and D), along with survival curves for the sham and organoid groups, failed to reveal any significant findings, indicating the lack of efficacy in the recovery of NSG mice using the APAP overdose model.

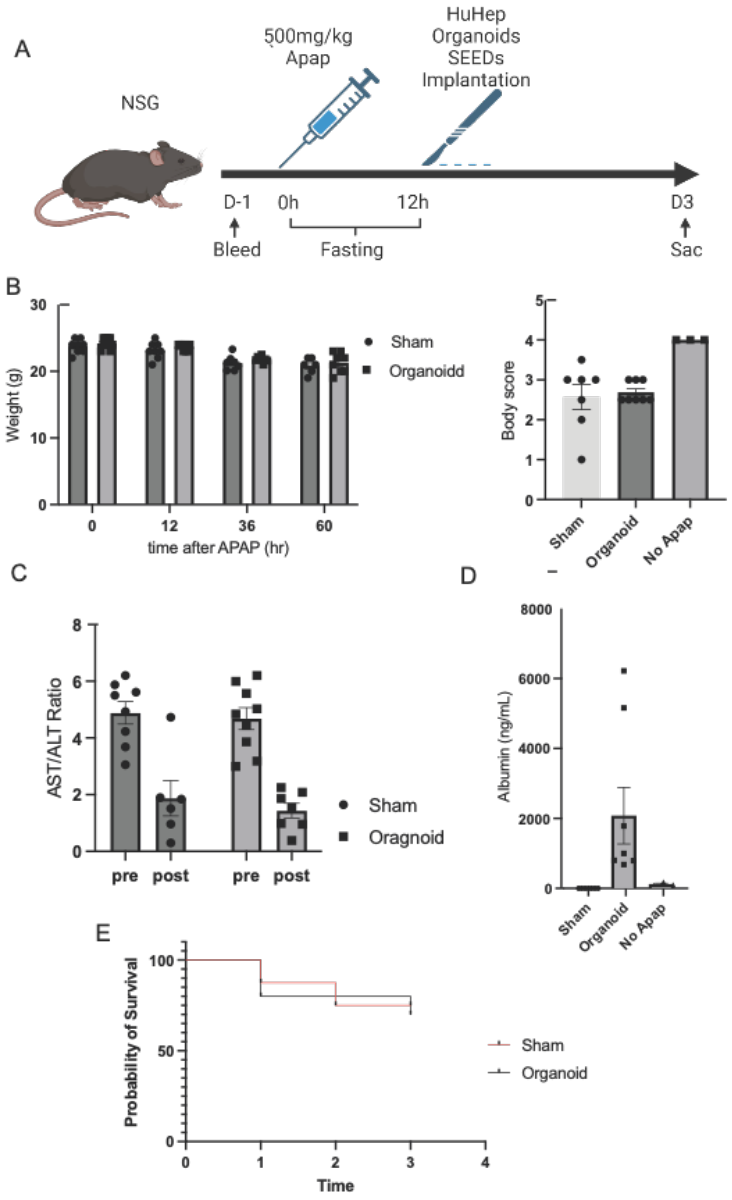

Figure 6.4: Investigation of Therapeutic Effects and Engraftment Potential of Organoids in APAP-Induced Liver Injury Model in NSG Mice using Engineered liver tissue seeds, 12 hour fasting period, and 500 mg/kg APAP

(A) Schematic of Approach for APAP-Induced Liver Injury Model in NOD-SCID IL2Rγ^null (NSG) Mice Utilizing Engineered Liver Tissue Seeds, a fasting period, and 500 mg/kg of APAP.

(B) Relationship between body weight and body score in NSG Mice.

(C) AST and ALT ratio measured in mouse blood. Data represented as mean +/- SEM of the sham and organoid groups at Day 5, pre and post APAP administration.

(D) Secreted human albumin measured in mouse blood by human albumin ELISA. Data represented as mean +/- SEM of the sham and organoid, and No APAP groups after 5 days.

(E) Survival Curve of Organoid transplanted and Sham NSG mice.

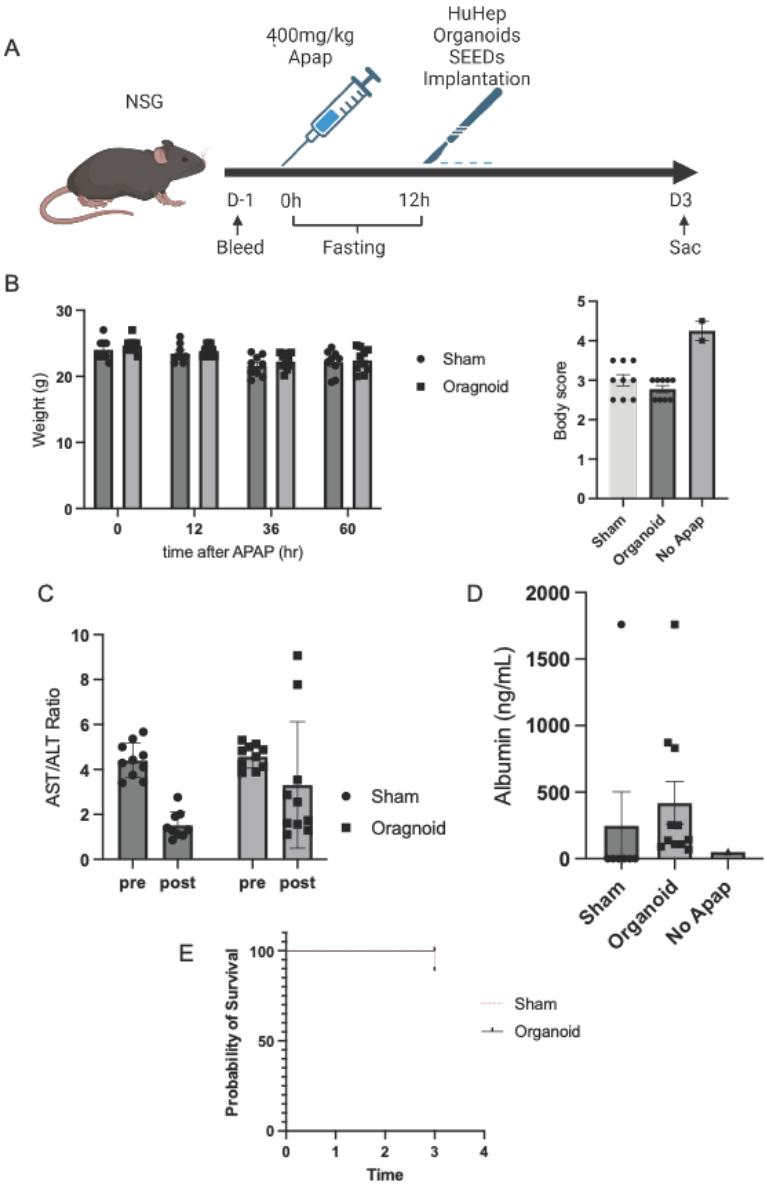

Figure 6.5: Investigation of Therapeutic Effects and Engraftment Potential of Organoids in APAP-Induced Liver Injury Model in NSG Mice using Engineered liver tissue seeds, 12 hour fasting period, and 400 mg/kg APAP

(A) Schematic of Approach for APAP-Induced Liver Injury Model in NOD-SCID IL2Rγ^null (NSG) Mice Utilizing Engineered Liver Tissue Seeds, a fasting period, and 400 mg/kg of APAP

(B) Relationship between body weight and body score in NSG Mice

(C) AST and ALT ratio measured in mouse blood. Data represented as mean +/- SEM of the sham and organoid groups at Day 5, pre and post APAP administration.

(D) Secreted human albumin measured in mouse blood by human albumin ELISA. Data represented as

mean +/- SEM of the sham and organoid, and No APAP groups after 5 days.

(E) Survival Curve of Organoid transplanted and Sham NSG mice.

6.3 DISCUSSION

The results of our experiment provide valuable insights into the induction of liver injury and recovery in NSG mice using two distinct methods of introducing adult human hepatocyte organoids. In the first approach, we integrated adult human hepatocyte organoids into engineered liver tissue seeds, implanted them into NSG mice and evaluated their response to APAP-induced liver injury. In the second approach, we injected the adult human hepatocyte organoids into the perigonadal fat pad of NSG mice to measure their therapeutic recovery. These two methods allowed us to assess the potential efficacy of our approach in mitigating drug-induced liver injury (DILI).

In the first model, where we induced liver injury using APAP and measured recovery through body weight and body scores, our findings suggest that the organoid-treated group exhibited a more favorable overall condition. The difference in body weight suggests that the organoid-treated mice experienced a less severe impact from the induced liver injury, supporting the notion that our approach has therapeutic potential. The body scores recorded at the peak of distress (36 hours after injury induction) further reinforced these findings. The organoid-treated mice displayed more favorable body scores, indicating a better overall condition compared to the sham group. These observations are encouraging, as they point towards a potential therapeutic benefit of utilizing adult human hepatocyte organoids integrated into engineered liver tissue seeds in the context of DILI.

The analysis of serum samples for liver injury markers, specifically Aspartate AST and ALT, revealed that the ratio of AST to ALT did not display significant differences between the organoid

and sham groups. This observation suggests that the extent of liver injury induced by Acetaminophen (APAP) was similar in both groups. It's important to note that there could be other potential explanations for this similarity, such as variations in the handling of serum samples, where some samples were found to be hemolyzed during processing, possibly leading to errors in the numerical values presented. Nevertheless, these results do not necessarily contradict our earlier findings, as the full therapeutic efficacy of our approach may not be adequately represented by these conventional markers alone.

The measurement of human albumin levels in the serum samples revealed a notable difference between the organoid-treated group and the sham group. The organoid-treated mice exhibited significantly higher levels of human albumin, indicating a more robust recovery response. This is a critical finding, as human albumin is an essential protein associated with liver function, and its increased levels suggest a more efficient restoration of liver function in the hepatocyte organoid group.

In addition to our first study involving the integration of adult human hepatocyte organoids into engineered liver tissue seeds, we conducted a second study utilizing a different approach. In this second study, we injected the adult human hepatocyte organoids into the perigonadal fat pad of NSG mice, providing an alternative model for assessing therapeutic recovery in the context of drug-induced liver injury (DILI).

To evaluate the recovery in this alternative model, we monitored two crucial parameters, body weight, and body scores. The body scores, which were recorded to assess the overall condition of the mice, revealed noteworthy differences between the organoid-treated group and the control

group injected with HBSS. The body scores in the organoid group indicated a more favorable overall condition when compared to the HBSS-injected control group. This suggests that the presence of the organoids may contribute to a better recovery response in this model.

Similar to the first study, we also collected serum samples at the end of the 5-day experimental period to measure AST and ALT liver injury markers. In this case, we found that the ratio did not exhibit significant differences between the organoid-treated and control groups, indicating a similar extent of liver injury. This result aligns with our observations from the first study, highlighting that the extent of liver injury induced in both models was comparable.

To further elucidate the potential of our approach, we also assessed the organoid-treated group alongside a control group that did not receive APAP (the "no APAP" group). It is important to note that the absence of APAP in the no APAP group had a noticeable impact on the recovery response, as indicated by higher human albumin levels. The comparison with the no APAP group highlights the influence of the drug-induced liver injury on the overall recovery response. Despite this variability, our results still support the therapeutic potential of the organoid approach, with some differences in recovery dynamics.

In summary, our second study, involving the injection of adult human hepatocyte organoids into the perigonadal fat pad of NSG mice, also demonstrated improved recovery responses, particularly in terms of body scores and human albumin levels, when compared to the control group. These findings further underscore the potential therapeutic benefits of our approach in mitigating drug-induced liver injury, while also highlighting some variability in recovery dynamics influenced by the presence or absence of the inducing agent (APAP). These results collectively contribute to our

understanding of the therapeutic potential of adult human hepatocyte organoids in the context of DILI and pave the way for further investigations and refinements in this area of research.

Our experiments involving the integration of adult human hepatocyte organoids into engineered liver tissue seeds and their subsequent injection into the perigonadal fat pad of NSG mice have yielded promising results. Notably, we have observed enhanced recovery responses in terms of improved body scores and elevated human albumin levels in mice treated with these organoid-containing liver tissue seeds. These findings suggest a potential therapeutic benefit of our approach in mitigating DILI.

The observed improvements highlight the significance of our method in promoting liver regeneration and function following injury. However, further research is needed to fully grasp the underlying mechanistic processes. Detailed studies of these mechanisms could provide insights into how transplanted organoids interact with the body's environment, clarifying their role in liver regeneration and repair processes.

Furthermore, refining our approach through additional experiments and optimizations has the potential the improve its efficacy and suitability for clinical use. This includes but is not limited to exploring different dosages, delivery methods, or combinations with other therapeutic interventions to maximize the therapeutic benefits while minimizing potential adverse effects.

In conclusion, our findings provide valuable insights into the potential of utilizing adult human hepatocyte organoids in engineered liver tissue seeds as a therapeutic strategy for DILI. Continued research and development hold the promise of advancing our understanding and

ultimately improving patient outcomes in liver disease management.

6.4 METHODS

6.4.1 *Organoid culture of hepatocytes*

Cryopreserved hepatocytes were thawed into 37°C medium and quickly spun down at 70 x g. Cells were mixed with 45% organoid media and 55% Matrigel and seeded in 20 µl droplets in each well of 48-well plates. After Matrigel had solidified, 200 µl of organoid medium was added to each well. Organoid medium: 40% Basal medium (DMEM/F12, 1x GlutaMAX, 1x HEPES, 1x penicillin-streptomycin, 2% B27, 10 mM nicotinamide, 1.25 mM N-acetyl cysteine, 10 nM gastrin), 50% Wnt3a conditioned medium, 10% Rspo1 conditioned medium, 50 ng/ml EGF, 5 µM A83-01, and 10 µM y-27632. Medium was refreshed every 2-3 days with care not to disturb the Matrigel droplet. Organoid size and growth were quantified from minimum intensity projections of brightfield z-stacks taken on a Nikon Eclipse Ti inverted high-resolution widefield microscope. Organoids were grown for 7 days.

6.4.2 *Organoid Dissociation*

Organoid fragments were prepared following 30 minutes of digestion in Cell Recovery solution on ice. After organoid digestion from Matrigel, cells are spun down at 70 x g. Organoids are resuspended in TrypLE and incubated for 5 minutes, strained with 70 µm cell strainer. Wash cell strainer with HBSS, 0.0025 mg/ml DNase I, 2% FBS (HBSS-DF) and rinse with HBSS, dropwise. Sediment cells at 70 x g for 5 minutes and resuspend in HBSS, followed by mechanical dissociation for hemocytometer quantification.

6.4.3 *Engineered liver tissue fabrication*

Hepatocyte organoids were digested out of Matrigel (Corning) with Cell Recovery Solution (Corning), washed once in PBS, and resuspended in diluted fibrinogen. Diluted thrombin was mixed with an equal volume of hepatocyte organoids in diluted fibrinogen and 60 ul was pipetted into 6mm PDMS gaskets. After 30 minutes of incubation, fibrin/cell gels were released from gaskets and implanted in mice as engineered liver tissue seeds. The final cell concentration was 2.1 million hepatocytes/ml. Fibrin was used at a final concentration of 10 mg/ml.

6.4.4 *Implantation and induction of liver injury*

All surgical procedures were conducted according to protocols approved by the University of Washington Institutional Animal Care and Use Committees. 6-week-old male NOD-SCID IL2Rγ^null (NSG) mice (Jackson) were administered APAP at 500 ug/kg of body weight, 12 hours before implantation or injection of organoids. Prior to surgery, NSG mice were administered sustained release buprenorphrine at least 1 hr prior to surgery in addition to local analgesic lidocaine and bupivacaine (1-2mg/kg) immediately prior to surgery and anesthetized with isofluorane.

Twelve engineered liver tissue seeds with or without organoids were sutured onto the perigonadal fat pads of each mouse. 1.5 million organoids were injected into the perigonadal fat pad of each mice receiving organoids, control mice received HBSS injections. Incisions were closed aseptically. After surgery, animals were subcutaneously injected with meloxicam (5-20 mg/kg) at least 30 minutes prior to recovery from the surgery, and then administered every 20-24 hours for 48 hours. Body weight was measured every day after the surgery until the mice were sacrificed. Body score was monitored by checking the mice behavior including the activity levels, ruffling of the fur, hunched position, and whether mice are actively grooming, eating, and

drinking, and rated from 1 (lethargic and morbid) to 5 (active and normal). Animals were sacrificed 3 days after implantation and injection of organoid tissues.

6.4.5 *Albumin ELISA*

Blood was drawn retro-orbitally for human albumin ELISA (Bethyl Laboratories) and immediately prior to sacrifice at the termination of the experiment. Serum was separated by centrifugation and levels of human albumin were determined by an enzyme-linked immunosorbent assay (ELISA) using goat polyclonal capture and horseradish peroxidase–conjugated goat anti- human albumin detection antibodies (Bethyl Laboratories).

6.4.6 *ALT/AST*

Blood was drawn retro-orbitally ALT and AST testing immediately prior to sacrifice at the termination of the experiment. Serum was separated by centrifugation and levels of AST and ALT were determined by core facilities (UW Comparative Medicine) and Moichor.

6.4.7 *Statistics*

Statistical analyses were performed with an Student t-test with unequal variance (Welch's correction). $P < 0.05$ was considered statistically significant.

Chapter 7: CCl4-Induced Liver Injury in NSG Mice Using Human Hepatocyte Organoids

7.1 Introduction

Liver injury is a significant health concern that can lead to severe complications, including fibrosis, cirrhosis, and even hepatocellular carcinoma. Carbon tetrachloride (CCl4) has been widely used as a model compound to induce fibrotic liver injury in animal models(72). Human hepatocyte organoids has been proposed to offer a more representative environment for studying liver pathophysiology compared to traditional animal models of liver injury(73). This chapter focuses on the utilization of human hepatocyte organoids to investigate CCl4-induced liver injury in NOD-SCID IL2Rγ^null (NSG) mice, highlighting their potential in bridging the gap between traditional animal models and human biology.

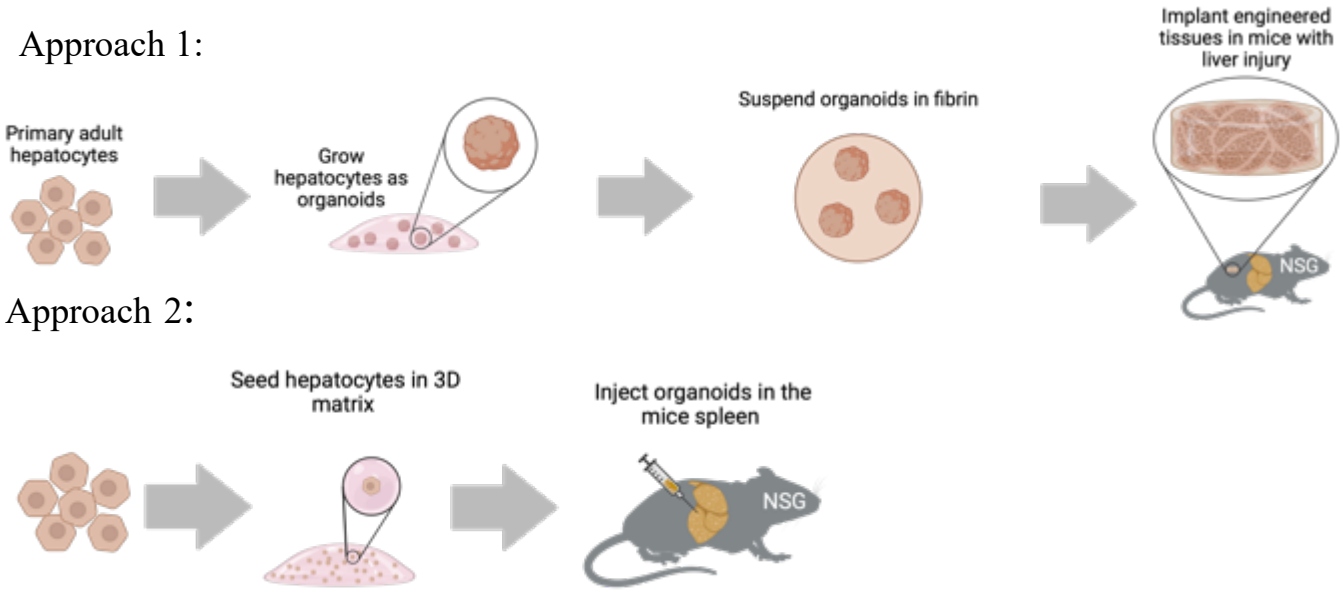

Figure 7.1: Schematic of Approaches for CCl4-Induced Liver Injury Model in NOD-SCID IL2Rγ^null (NSG) Mice Utilizing Engineered Liver Tissue Seeds and Intrasplenic Injections

7.2 RESULTS

We chose to examine two approaches to analyze the CCl4 induced liver injury model.

7.2.1 *Engineered liver tissue seeds*

We conducted an experiment to assess the impact of carbon tetrachloride (CCl4) on liver injury in NSG mice, using human hepatocyte organoids within engineered liver tissue seeds. Specifically, we examined the response of transplanted hepatocyte organoids to CCl4 treatment after 30 days, employing various methods to evaluate liver function, fibrosis, and hepatocellular damage.

To assess the engraftment potential of hepatocytes grown as organoids in engineered tissue seeds, we cultured adult human hepatocytes for seven days and encapsulated them within fibrin hydrogels, creating engineered liver tissue seeds and then implanted into the perigonadal fat pad of NSG (NOD-SCID IL2Rγ^null) mice, which are immunocompromised and lack mature T, B, and functional NK cells and thus can receive xenograft implants. These mice are known to be more susceptible to CCl4-induced liver damage and fibrosis.

We conducted tests to measure the levels of alanine transaminase (ALT) and aspartate aminotransferase (AST) enzymes in the collected blood at week 2 and week 4, as these enzymes are primarily found in the liver and can indicate liver damage or disease. Interestingly, we observed a decrease in the ratio of AST to ALT over the 30-day period in vivo. In a healthy liver, ALT levels are typically higher than AST levels, resulting in a low AST/ALT ratio. When liver cells are damaged, ALT is released into the bloodstream in greater quantities than AST, causing an increase in the ALT level and a decrease in the AST/ALT ratio. This pattern is often seen in cases of acute liver injury (70). Our study suggests that, over time, the mice experienced less severe liver damage, indicating that more initial injury might be required for a conclusive study (Figure 7.1 F),

Subsequently, we performed Hematoxylin and Eosin, (H&E), Sirius Red (SR) and Fast Green (FG) staining on sectioned explanted liver tissue, revealing elevated collagen fiber levels throughout the liver tissues. Increased collagen deposition is a characteristic feature of fibrotic conditions (Figure 7.2 C-D). To quantify the liver injury, measurements were taken from Sirius Red and Fast Green histochemical stains (Figure 7.2B). Furthermore, when we examined excised engineered liver tissue seed grafts from the NSG mice, we observed large areas where most cells stained positive for a hepatocyte marker, Cytokine 18 (CK 18) (Figure 7.2 E). This demonstrates that, although we did not induce significant liver injury, engraftment of hepatocytes from xenograft implants did occur.

To confirm the functionality of the transplanted hepatocyte organoids within the engineered liver tissue, we conducted measurements of human albumin levels after a 30-day period (Figure 7.2A). The results of this analysis were particularly striking, revealing a substantial 16-fold elevation in human albumin levels when comparing the group that received the human hepatocyte organoid engineered liver tissue seeds to the control group. This marked increase in human albumin levels provides strong evidence of the robust functionality of the grafted cells within the engineered liver tissue. The significant rise in human albumin levels suggests that the hepatocyte organoids not only successfully engrafted but also retained their capacity to produce albumin.

In summary, our findings indicate that utilizing adult human hepatocytes as organoids within engineered liver tissue seeds allows for the engraftment and propagation of cells that closely resemble human hepatocytes in terms of morphology, phenotype, and function. However, this approach did not contribute to the mitigation of liver injury in the CCl4 liver injury model.

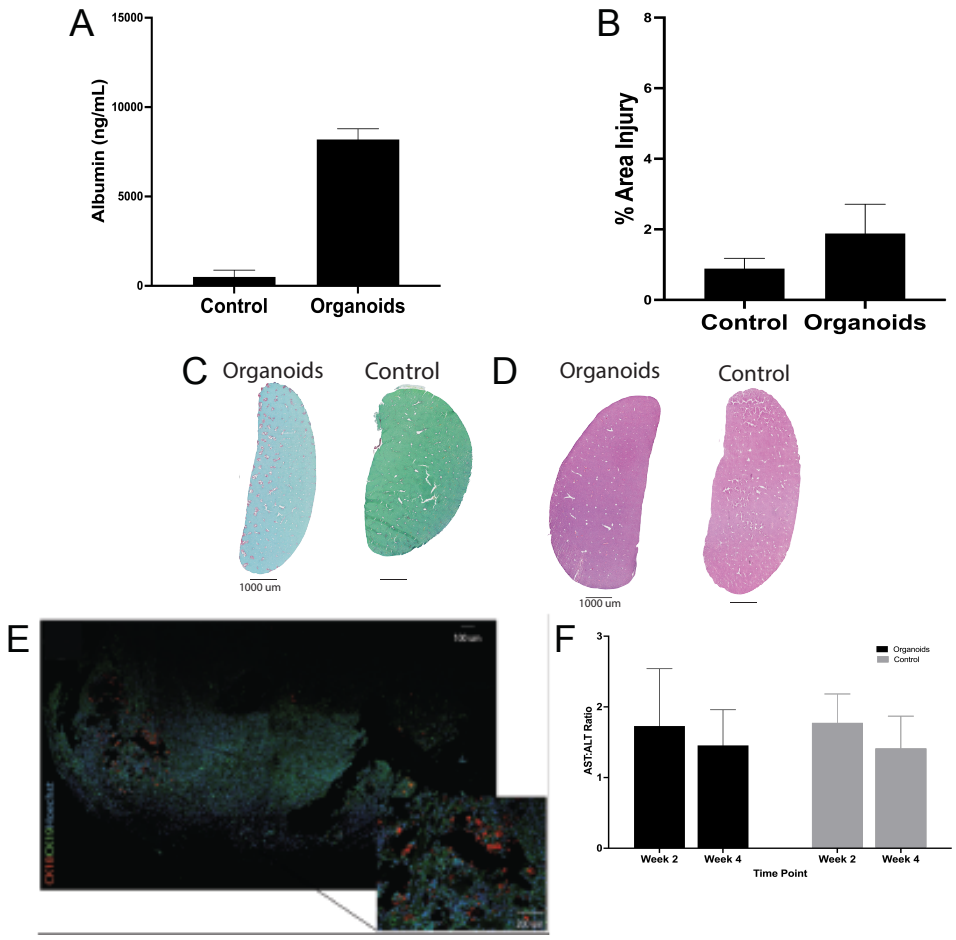

Figure 7.2: Investigation of Therapeutic Effects and Engraftment Potential of Organoids in CCl4-Induced Liver Injury Model in NSG Mice using Engineered liver tissue seeds

(A) Secreted human albumin measured in mouse blood by human albumin ELISA. Data represented as mean +/- SEM of the control and organoid groups after 30 days.

(B) Percentage of Injured Area based on histochemical images of explanted liver graft stained for Sirius Red and Fast Green. Data represented as mean +/- SEM of the control and organoid groups.

(C) Percentage of Injured Area based on histochemical images of explanted liver graft stained for Sirius Red and Fast Green. Data represented as mean +/- SEM of the control and organoid groups.

(D) Histochemical images of explanted liver graft stained for Sirius Red and Fast Green. Low magnification scale bar = 1000 µm

(E) ≈ Immunofluorescence image of explanted engineered liver tissue seeds stained against CK18 (red), CK19 (green), and Hoechst (blue). Low magnification scale bar = 100 µm, inset scale bar = 200 µm

(F) AST and ALT ratio measured in mouse blood. Data represented as mean +/- SEM of the control and organoid groups after Week 2 and Week 4.

7.2.2 *Intrasplenic Injection*

In conjunction with the engineered liver tissue seeds, we employed intrasplenic injection of organoids with identical parameters of the CCl4 liver injury model to investigate the therapeutic effects of recovery using organoids. This delivery method lacked a biocompatible matrix surrounding the organoids, thereby affording direct access for the organoids to navigate the spleen and subsequently engraft in the liver. It is worth noting that the use of intrasplenic injection required a reduction in the number of cells transplanted; for this specific experiment, we injected 0.5 million human hepatocytes cultured as organoids for a duration of 7 days.

To evaluate the engraftment potential, we conducted histochemical staining, specifically Sirius Red, Fast Green and H&E staining, on both freshly thawed cryovial cells and injured mice (Figure 7.3D- E). Notably, our analysis revealed no discernible differences. H&E stain comprises Hematoxylin and Eosin, two dyes used to visualize nuclei and proteins of the stained tissue which allows for the examination of various elements of the tissues, including nuclei, cytoplasm, muscle fibers, red blood cells, calcium, and mucin(74). We used H&E staining to visualize changes in hepatocyte morphology, identify areas of inflammation and fibrosis, and gain insights into the extent of liver damage, providing valuable histopathological information in the context of our study. To quantify the liver injury, measurements were taken from Sirius Red and Fast Green histochemical stains (Figure 7.3B).

Given the absence of significant disparities in histochemical staining outcomes, we proceeded to quantify the levels of AST and ALT to determine the presence of any fibrotic activity (Figure 7.3C). AST and ALT are well-established biomarkers commonly utilized in assessing liver function and injury. Our findings revealed intriguing results; while in the control mice, the

AST/ALT ratio exhibited a noticeable increase, indicative of possible liver stress or injury, no such alteration was observed in the treated mice. This differential pattern in enzyme activity between the control and treated groups provides valuable information about the impact of the experimental intervention on hepatic health, further enhancing our understanding of the liver's response to the investigated conditions.

Subsequently, considering the inconclusive results, we sought to confirm the liver function of both the freshly thawed cryovial cells (control) group and the organoid-treated group. We collected serum samples at day 30 to measure the production of human albumin in the mice (Figure 7.3A). Notably, the cryo control group exhibited a marked disparity in albumin production levels compared to the organoid group. These findings suggest that organoid treated groups have slower engraftment compared to freshly thawed hepatocytes used in cryo control groups. One of the potential technical issues between the two groups are accurate enumeration of cell numbers. In the case of freshly thawed cells, the ability to individually count single cells facilitated an accurate determination of the cell count for injection. Conversely, organoids formed clusters that posed challenges for enumeration without dissociation. We speculate that the number of cells plated did not result in the generation of additional cells, thereby enabling us to conclude that the quantity of cells at the time of collection remained consistent.

As we consider future steps in our research, we propose a direct comparison between organoids and a saline solution, such as Hank's Balanced Salt Solution (HBSS) from Thermo Fisher. This approach would enable a more precise evaluation of the therapeutic effectiveness of organoids in comparison to a blank control. This methodology would alleviate the need for normalization of cell numbers, a challenge that arises when comparing the count of freshly thawed cells to that of

organoids.

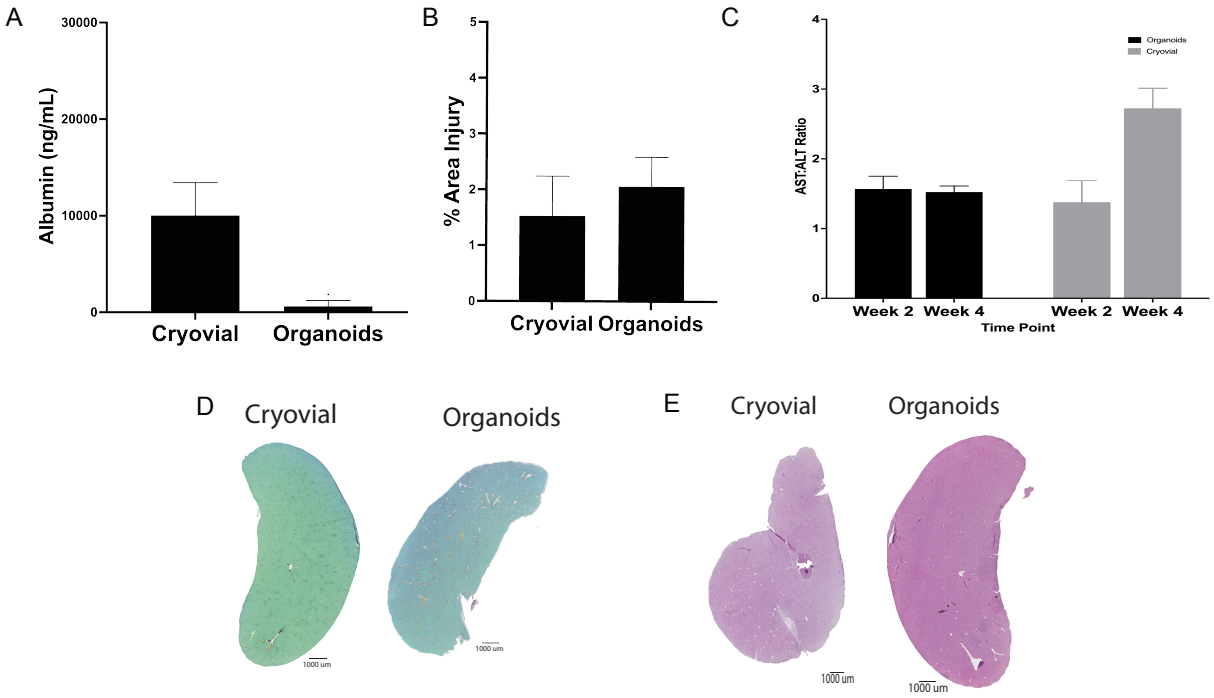

Figure 7.3: Investigation of Therapeutic Effects and Engraftment Potential of Organoids in CCl4-Induced Liver Injury Model in NSG Mice using Intrasplenic Injection

(A) Secreted human albumin measured in mouse blood by human albumin ELISA. Data represented as mean +/- SEM of the freshly thawed cryovial cells and organoid groups after 30 days.

(B) Percentage of Injured Area based on histochemical images of explanted liver graft stained for Sirius Red and Fast Green. Data represented as mean +/- SEM of the control and organoid groups.

(C) AST and ALT ratio measured in mouse blood. Data represented as mean +/- SEM of the freshly thawed cryovial cells and organoid groups after Week 2 and Week 4.

(D) Histochemical images of explanted liver graft stained for Sirius Red and Fast Green. Low magnification scale bar = 1000µm.

(E) Histochemical image of explanted liver graft stained for H&E. Low magnification scale bar = 1000µm.

7.3 DISCUSSION

Our research is aimed to explore the utilization of human hepatocyte organoid cultures offers a novel method for maintaining function of human hepatocytes in culture for engraftment, thereby augmenting hepatocyte effectiveness in terms of phenotype, morphology, function, and maturity. In this study, we demonstrated that human hepatocyte organoids cultured *in vitro* were subsequently implanted as xenografts and successfully engrafted in immunocompromised NSG mice *in vivo*.

We did not see the impact of organoids in CCl4 induced liver fibrosis most likely because the injury was too mild at the initial concentration of 1uL/g of body weight. The AST/ALT readings are affected by hemolysis which may have been a factor in our analysis. We missed the peak injury time and thus histology is not conclusive either.

While our study did not yield definitive conclusions, it did provide potential of human hepatocytes on therapeutic efficacy through liver engraftment in these mice. This finding prompts a comparison with alternative methods for hepatocyte engraftment, particularly when considering intrasplenic injection and the use of artificial liver tissue seeds.

We wanted to compare the two human hepatocyte organoid delivery methods, intrasplenic injections vs engineered liver tissue seeds, which has their own merits. Intrasplenic injection has been a well-established method for hepatocyte transplantation. It involves direct injection of hepatocytes into the spleen, where they can subsequently migrate and engraft in the liver, its native environment optimized for its function, However, this method has limitations, including the risk of portal hypertension and hepatic ischemia, which can lead to complications and reduced

engraftment efficiency (75) and the number of cells that can be injected are limited. Our study suggests that the use of hepatocyte organoid cultures may offer an alternative with a potentially superior engraftment mechanism, although further investigation is needed to directly compare these methods.

On the other hand, the artificial liver tissue seeds, formed using fibrin and thrombin, represent an innovative approach to hepatocyte transplantation. This technique allows for the encapsulation of hepatocytes within a biocompatible matrix before transplantation. While this approach may offer benefits such as controlled release of hepatocytes and a mechanism to transfer human hepatocytes in large numbers to the mice.

The results obtained from our study, including the assessment of albumin levels, immunofluorescence imaging, and brightfield quantification, collectively suggest that the implanted and injected cells exhibit characteristic similarities to human liver cells. Intrasplenic injection of freshly thawed cryovial cells engrafts in the liver better than organoid injection. However, organoid injected groups show improved AST/ALT ratio which suggests that the organoids may have potential for ameliorating fibrotic liver injury despite slower engraftment as suggested by lower levels of albumin.

Immunofluorescence imaging and brightfield quantification provide visual and quantitative evidence of the cells' resemblance to native human liver tissue. These findings underscore the potential of hepatocyte organoid cultures as a promising avenue for hepatocyte engraftment in therapeutic applications.

Our study highlights the potential of hepatocyte organoid cultures to enhance hepatocyte engraftment, offering promise for enhancing the effectiveness of liver transplantation therapies. However, to fully understand the therapeutic implications of CCl4 treatment, further research is warranted, involving the exploration of increased concentration levels and adjustments to the injection timing. As liver cell therapy advances toward clinical applications, ongoing improvements such as the generation of adult human hepatocyte organoids at scales relevant to human organs will expedite translation to the clinic. The adult human hepatocyte organoids described in this study have the potential to significantly advance both basic and clinical research across various domains, including therapeutic regenerative medicine, pharmaceutical screening, and the development of patient-specific organoids for precision medicine.

7.4 METHODS

7.4.1 *Organoid culture of hepatocytes*

Cryopreserved hepatocytes were thawed into 37°C medium and quickly spun down at 70 x g. Cells were mixed with 45% organoid media and 55% Matrigel and seeded in 20 µl droplets in each well of 48-well plates. After Matrigel had solidified, 200 µl of organoid medium was added to each well. Organoid medium: 40% Basal medium (DMEM/F12, 1x GlutaMAX, 1x HEPES, 1x penicillin-streptomycin, 2% B27, 10 mM nicotinamide, 1.25 mM N-acetyl cysteine, 10 nM gastrin), 50% Wnt3a conditioned medium, 10% Rspo1 conditioned medium, 50 ng/ml EGF, 5 µM A83-01, and 10 µM y-27632. Medium was refreshed every 2-3 days with care not to disturb the Matrigel droplet. Organoid size and growth were quantified from minimum intensity projections of brightfield z-stacks taken on a Nikon Eclipse Ti inverted high-resolution widefield microscope. Organoids were grown for 7 days.

7.4.2 *Engineered liver tissue fabrication*

Hepatocyte organoids were digested out of Matrigel (Corning) with Cell Recovery Solution (Corning), washed once in PBS, and resuspended in diluted fibrinogen. Diluted thrombin was mixed with an equal volume of hepatocyte organoids in diluted fibrinogen and 60 ul was pipetted into 6mm PDMS gaskets. After 30 minutes of incubation, fibrin/cell gels were released from gaskets and implanted in mice as engineered liver tissue seeds. The final cell concentration was 2.1 million hepatocytes/ml. Fibrin was used at a final concentration of 10 mg/ml.

7.4.3 *Organoid Dissociation*

Organoid fragments were prepared following 30 minutes of digestion in Cell Recovery solution on ice. After organoid digestion from Matrigel, cells are spun down at 70 x g. Organoids are resuspended in TrypLE and incubated for 5 minutes, strained with 70 μm cell strainer. Wash cell strainer with HBSS, 0.0025 mg/ml DNase I, 2% FBS (HBSS-DF) and rinse with HBSS, dropwise. Sediment cells at 70 x g for 5 minutes and resuspend in HBSS, followed by mechanical dissociation for hemocytometer quantification.

7.4.4 *Implantation and induction of liver injury*

All surgical procedures were conducted according to protocols approved by the University of Cambridge Institutional Animal Care and Use Committees. 4-week-old male NOD-SCID IL2Rγ^null (NSG) mice (Charles River) were administered CCL4 at 1uL/g of body weight, allowing the mice to receive 2-3 doses per week until 2 days prior to injection. NSG mice were then administered sustained release buprenorphrine and anesthetized with isofluorane.

Twelve organoid engineered liver tissue seeds were sutured onto the perigonadal fat pads of each mouse. Eight mice received organoid fibrin seeds and six mice received sham fibrin seeds. 500K

organoids were injected into the spleen of each mice receiving organoids; six mice received HBSS injections, and six mice received organoid injections. Incisions were closed aseptically. Animals were sacrificed 30 days after implantation and injection of organoid tissues.

7.4.5 *Albumin ELISA*

Blood was drawn from the superficial tail vein for human albumin ELISA (Bethyl Laboratories) and immediately prior to sacrifice at the termination of the experiment (30 days). Serum was separated by centrifugation and levels of human albumin were determined by an enzyme-linked immunosorbent assay (ELISA) using goat polyclonal capture and horseradish peroxidase–conjugated goat anti- human albumin detection antibodies (Bethyl Laboratories).

7.4.6 *ALT/AST*

Blood was drawn from the superficial tail vein for ALT and AST testing at 2 weeks and immediately prior to sacrifice at the termination of the experiment (30 days). Serum was separated by centrifugation and levels of AST and ALT were determined by core facilities (University of Cambridge).

7.4.7 *Tissue harvesting and organoid histology*

Organoid tissues were identified using the surgical suture as a landmark then were excised and fixed in 4% paraformaldehyde (PFA) for 48 hours at 4°C. Excess fat was removed from around the implant. Trimmed grafts were then dehydrated, paraffin-embedded, and sectioned on a microtome (5-20 mm sections).

7.4.8 *Histochemical staining, immunofluorescent staining, and microscopy*

Histochemical staining of organoids was performed with Hematoxylin and eosin (H&E), Sirius Red and Fast Green, and Trichome; conducted by the histology core at University of Washington ISCRM Facility.

Immunofluorescence staining of organoids was performed by deparaffinizing sections, performing antigen retrieval, blocking with normal donkey serum for 1 hour at room temperature, then incubating with primary antibody overnight at 4°C. The following day, sections were washed with PBS-T and then incubated with secondary antibody + Hoechst 33342 (Thermo H3570) for 1 hour at room temperature, washed, and mounted with Fluoromount-G (Invitrogen). All antibody information is included in Table 1. Images were obtained using a Nikon Eclipse Ti inverted high-resolution widefield microscope, or a Nikon A1R scanning confocal microscope. Images were processed using Adobe Photoshop or ImageJ software. For morphometric analyses, images were thresholded and pixels were measured using ImageJ software.

7.4.9 *Statistics*

Statistical analyses were performed with an unpaired t-test with unequal variance (Welch's correction). $P < 0.05$ was considered statistically significant.

Chapter 8. CONCLUSION

8.1 SUMMARY OF CURRENT WORK

The liver, the largest solid organ in the human body, is pivotal in maintaining homeostasis through its multifaceted functions (76). Notably, the liver detoxifies the bloodstream, influencing the body's tolerance to toxic substances (77). Drug-induced liver injury (DILI) is a significant concern, as it can lead to severe liver failure and even mortality, underscoring the importance of understanding how the liver responds to toxins and medications. With the global burden of liver disease rising, liver transplantation remains the primary curative option for late-stage cases (26), yet the shortage of available organs persists.

The liver's remarkable capacity, though present, has not been successfully replicated to stably culture and propagate human hepatocytes *ex vivo* (78). To address this challenge, our research explores the use of organoid culture as a promising method for cultivating hepatic cells and modeling the human liver *in vitro*. Establishing a reliable *in vitro* culture system for human hepatocytes holds great promise for advancing our understanding of human liver regeneration, drug metabolism, and hepatotoxicity (79,80).

Furthermore, our work showcases the potential to therapeutically rescue mice with liver damage, offering a potential bridge therapy or alternative to whole organ transplantation. Ultimately, this research has the potential to provide a valuable human liver model, aiding researchers in gaining insights into the intricate processes of liver biology and paving the way for innovative solutions in the field of liver disease treatment.

In the first section, we characterized the extent to which human hepatocyte organoids can be expanded *in vitro*. Chapter 2 expounded upon our ability to analyze hepatocyte proliferation in our current media formulation. Specifically, we compared the proliferation rates between Day 7 and Day 14 organoids. Our analysis revealed a higher rate of hepatocyte proliferation at Day 7. However, by Day 14, we observed a decrease in hepatocyte proliferation, with a predominant presence of proliferative biliary cells, including cholangiocytes. This observation strongly suggested a noticeable shift in the pattern of cell proliferation over time. The findings provided an avenue for examination of whether the proliferation shift was due to the current culture medium.

To expound on the media formulation, in Chapter 3, we analyzed multiple formulations and combinations of growth factors and small molecules known to affect the growth of the hepatocyte organoids. We first tested original formulations previously used in developing the hepatocyte organoids. Results showed that A83-01 was a main component in the growth and function of the hepatocyte organoids. We further tested multiple concentrations to determine the optimal concentration for optimal functionality and size. Ultimately concluded that the inhibition of TGF-β at the higher concentrations was not beneficial for the functionality and size of the organoids, and that further studies are necessary to fully determine the effects of TGF-β. In summary, our study involved an analysis of TGF-β, activation and inhibition. We observed that the activation of TGF-β, had an insignificant effect on the production of higher-functioning hepatocyte organoids when compared to use of A83-01, a TGF-β inhibitor.

In Chapter 4, our focus shifted to the purification of adult human hepatocyte organoids using magnetic-activated cell sorting techniques, with the aim of extending the functionality of these hepatocytes. Two distinct

methodologies, Miltenyi and STEMCELL, were employed to culture and sort the hepatocytes. Our results demonstrated that the Miltenyi sorting approach led to higher functionality in the resulting hepatocyte organoids. Additionally, we explored the use of cell dissociation solutions and tested various combinations of passaging and sorting techniques to identify the most effective approach for generating highly functional human hepatocyte organoids. To assess the functionality of these organoids, we conducted direct measurements of liver function using various parameters, such as human albumin secretion and immunofluorescence staining. Our findings revealed that adult human hepatocytes exhibited robust maintenance of hepatic functions when subjected to organoid culture and were passaged and sorted at early time points. This observation suggests that the selected combination of passaging and sorting techniques significantly contributes to the long-term functionality of the human hepatocyte organoids.

In Chapter 5, our exploration of human hepatocyte organoids for therapeutic applications led us to utilize immunodeficient FNRG mice to investigate whether these organoids could successfully repopulate the livers. We tracked the mice over a span of 130 days to determine if their livers exhibited humanization as a result of intrasplenic injection of the hepatocyte organoids in comparison to the gold standard for the humanization used for these mice, which are freshly thawed cryopreserved human hepatocytes. Our primary marker for organoid functionality was the tracking of human albumin levels in serum. Our findings strongly indicated that the organoids demonstrated functional capacity similar to that of the control group, freshly thawed cryopreserved human hepatocytes. Notably, we observed that the organoids effectively engrafted and expanded within the livers of the FNRG mice at levels comparable to those achieved with freshly thawed cryopreserved human hepatocytes. An extended study involved transplanting passaged organoids and conducting a survival analysis on freshly grown organoids, comparing them to a control group of sham mice injected with HBSS. Unfortunately, due to issues related to the NTBC cycling process, which is responsible for liver injury in this model, we were unable to obtain conclusive results regarding long-term outcomes in this murine model.

Subsequently, our research endeavors shifted towards therapeutic applications. In Chapter 6, we embarked on establishing a model that combined an acetaminophen (APAP) mouse model with NSG immunocompromised mice. This involved the injection of APAP into the mice and the introduction of organoids into the perigonadal fat pad or the surgical grafting of engineered liver tissues onto the perigonadal fat of NSG mice. Our observations following APAP administration revealed that the utilization of adult human hepatocyte organoids integrated into engineered liver tissue seeds resulted in improved recovery, as evidenced by reduced morbidity, body scores and body weight, and increased levels of human albumin. Similarly, adult human hepatocyte organoids injected into the perigonadal fat pad of NSG mice exhibited enhanced recovery in terms of morbidity (body scores and body weight) and human albumin levels when compared to the control group. These findings underscore the potential therapeutic benefits of our approach in mitigating drug-induced liver injury and promoting liver recovery.

In Chapter 7, we employed the CCl4 model in NSG mice. The mice were administered CCl4, a known hepatotoxin, and organoids were introduced either via injection into the spleen or through surgical grafting of engineered liver tissues onto the perigonadal fat pad of the NSG mice. Our findings indicate that utilizing adult human hepatocytes as organoids within engineered liver tissue seeds allows for the engraftment and propagation of cells that closely resemble human hepatocytes in terms of morphology, phenotype, and function. However, utilizing intrasplenic injection, organoid treated groups have slower engraftment compared to freshly thawed hepatocytes used in cryo-preserved control groups and, ultimately, are less functional. Consequently, the organoid-treated groups demonstrated reduced functionality in comparison.

Despite this, the results from these therapeutic rescue studies are highly promising, showcasing that adult human hepatocyte organoids can serve as a valuable cell source for liver tissue

engineering. This approach opens a new avenue for the treatment of both acute and chronic liver diseases, which could have a transformative impact on human health and significantly enhance the field of liver therapeutics.

8.2 REMAINING CHALLENGES AND FUTURE DIRECTIONS

Despite significant advancements in liver tissue engineering, a critical challenge for clinical translation remains the scarcity of hepatocytes. While organoid culture shows promise in temporarily expanding adult human hepatocytes for transplantation, their limited long-term proliferative capacity hinders large-scale production required for clinical applications. To address this barrier and facilitate mass hepatocyte organoid generation, it is crucial to adapt organoid culture for high-throughput manufacturing, best suited for dedicated industrial facilities. Experimental efforts should focus on inducing prolonged organoid growth and passage-ability, allowing for exponential expansion of the initial cell population, and enabling applications such as drug toxicity testing. These developments hold the potential to make liver tissue engineering more feasible and transformative for the treatment of liver diseases in the clinical setting.

8.2.1 *Growth factors mechanisms affect human hepatocyte organoids*

Primary human hepatocytes have been grown in an organoid media optimized for hepatic organoid growth. Growth, phenotype, and function of organoids are heightened when grown with certain growth factors. To expand organoid research, samples have been probed for A83-01, an inhibitor of TGFβ, Receptor 1. The media has been optimized but it has been shown that A83-01 controls the TGFβ, signaling pathway and has great importance on organoid growth, so we want to optimize it. The results in this thesis, serve as a baseline for more expansion to optimizing organoid growth media for longer expansion of hepatocyte growth. There are many other factors that still need to

be identified that are differentially expressed and affect organoid growth via the growth media and apply them to *in vitro* hepatocyte organoids growth. Testing the hypothesis that mimicking the *in vivo* signaling factors in *in vitro* organoid culture will promote hepatocyte organoids to exhibit more mature gene expression and function. Future studies include testing growth factors (HGF, EGF, FGF15, FGF21, and TGFβ) at different concentration combinations and inflammatory cytokines (TNFα, IL6, and Oncostatin M) via High-throughput screening. It is thought that these growth factors stimulate regenerative signaling to help the efficacy of the organoids.

8.2.2 *High-throughput screening system for organoid testing*

High-throughput screening (HTS) combines the use of robotics and laboratory automation, building a system ideal for testing multiple variables in one efficient system. The system allows for studies of complex biological systems and drug therapeutics to be tested in timeframes that were once improbable. The focus is to optimize the organoids to be compatible with HTS. Currently, organoid growth is tedious causing greater experimental error. The organoids are grown in 48 well plates; for HTS optimization, organoids would need to be plated in slab gels in 384 well plates. Increasing the sample size, could cause variation in the growth process, which would need complete optimization to ensure the organoids growth stays consistent with the original 48-well plate method. Once organoids are compatible with HTS, endpoints relevant to toxicity, including viability assays (CellTiter GLO or Alamar blue) and growth (brightfield imaging), would be conducted.

8.2.3 *Prediction of drug toxicology on hepatic phenotype using HTS*

The optimized organoids grown would be used to begin to explore drug induction. Drugs being screened include *Amoxicillin-clavulanate, Isoniazid, RIP + INH + PIZ, Flutamide, and Ibuprofen* (80); the five most common drugs associated with liver injury, Acetaminophen; when used as directed, is extremely safe even for people with liver disease, and Herbal Antioxidants; which

impact to the liver is unknown. The endpoints optimized in HTS for toxicity, would be used, and this work will ultimately propel the lab forward in the mission to develop a renewable hepatocyte organoid model and will improve understanding of the mechanisms that control liver regeneration and disease. This work will determine the role of drug toxicity in adult human hepatocytes and the effects of hepatocyte organoid growth and maturity. The hope is that the HTS system will promote organoid proliferation and answer unknowns to the central challenge of disease modeling and drug discovery while maintaining organoid function, maturity, and phenotype. This work will be immediately relevant for drug developers and the pharmaceutical industry, speeding the drug development pipeline and helping to identify safe drug formulations.

The work summarized here demonstrates significant progress for liver tissue engineering. It opens many new possibilities for exciting research into the biology, pathology, and therapeutic applications of mature hepatocytes in the human liver.

BIBLIOGRAPHY

1. Zong Y, Stanger BZ. Molecular mechanisms of liver and bile duct development. Wiley Interdiscip Rev Dev Biol [Internet]. 2012 Sep 1 [cited 2023 Oct 24];1(5):643–55. Available from: https://onlinelibrary.wiley.com/doi/full/10.1002/wdev.47

2. Abdel-Misih SRZ, Bloomston M, Bismuth H. Liver Anatomy. 2010;

3. Lautt WW. Overview. 2009 [cited 2023 Oct 30]; Available from: https://www.ncbi.nlm.nih.gov/books/NBK53069/

4. Chen F, Schönberger K, Tchorz JS. Distinct hepatocyte identities in liver homeostasis and regeneration. JHEP Reports [Internet]. 2023 Aug 1 [cited 2023 Oct 30];5(8):100779. Available from: /pmc/articles/PMC10339260/

5. Cast AE, Walter TJ, Huppert SS. Vascular patterning sets the stage for macro and micro hepatic architecture. Dev Dyn [Internet]. 2015 Mar 1 [cited 2023 Oct 30];244(3):497. Available from: /pmc/articles/PMC4858172/

6.

6. Turcotte S. Chapter 5 - Liver blood flow: Physiology, measurement, and clinical relevance. Blumgart's Surgery of the Liver, Biliary Tract and Pancreas: Sixth Edition. 2016 Dec 2;1–2:77-92.e5.

7. Tanimizu N, Kaneko K, Itoh T, Ichinohe N, Ishii M, Mizuguchi T, et al. Intrahepatic bile ducts are developed through formation of homogeneous continuous luminal network and its dynamic rearrangement in mice. Hepatology [Internet]. 2016 Jul 1 [cited 2023 Oct 30];64(1):175–88. Available from: https://pubmed.ncbi.nlm.nih.gov/26926046/

8. Hundt M, Wu CY, Young M. Anatomy, Abdomen and Pelvis: Biliary Ducts. StatPearls [Internet]. 2023 Jul 15 [cited 2023 Oct 30]; Available from: https://www.ncbi.nlm.nih.gov/books/NBK459246/

9. Boyer JL. Bile Formation and Secretion. Compr Physiol [Internet]. 2013 [cited 2023 Oct 30];3(3):1035. Available from: /pmc/articles/PMC4091928/

10. Maroni L, Haibo B, Ray D, Zhou T, Wan Y, Meng F, et al. Functional and Structural Features of Cholangiocytes in Health and Disease. Cell Mol Gastroenterol Hepatol [Internet]. 2015 Jul 1 [cited 2023 Oct 30];1(4):368. Available from: /pmc/articles/PMC4530547/

11. Banales JM, Huebert RC, Karlsen T, Strazzabosco M, LaRusso NF, Gores GJ. Cholangiocyte pathobiology. Nat Rev Gastroenterol Hepatol [Internet]. 2019 May 1 [cited 2023 Oct 30];16(5):269. Available from: /pmc/articles/PMC6563606/

12. Michalopoulos GK. Liver regeneration. J Cell Physiol [Internet]. 2007 Nov [cited 2023 Oct 24];213(2):286–300. Available from: https://pubmed.ncbi.nlm.nih.gov/17559071/

13. Fausto N, Campbell JS, Riehle KJ. Liver regeneration. Hepatology [Internet]. 2006 Feb [cited 2023 Oct 24];43(2 Suppl 1). Available from: https://pubmed.ncbi.nlm.nih.gov/16447274/

14. Lorenz L, Axnick J, Buschmann T, Henning C, Urner S, Fang S, et al. Mechanosensing by β1 integrin induces angiocrine signals for liver growth and survival. Nature [Internet]. 2018 Oct 4 [cited 2023 Oct 24];562(7725):128–32. Available from: https://pubmed.ncbi.nlm.nih.gov/30258227/

15. Braet F, Shleper M, Paizi M, Brodsky S, Kopeiko N, Resnick N, et al. Liver sinusoidal endothelial cell modulation upon resection and shear stress in vitro. Comp Hepatol [Internet]. 2004 Sep 1 [cited 2023 Oct 24];3:7. Available from: /pmc/articles/PMC519024/

16. Ding B Sen, Nolan DJ, Butler JM, James D, Babazadeh AO, Rosenwaks Z, et al. Inductive angiocrine signals from sinusoidal endothelium are required for liver regeneration. Nature [Internet]. 2010 Nov 11 [cited 2023 Oct 24];468(7321):310–5. Available from: https://pubmed.ncbi.nlm.nih.gov/21068842/

17. Shimizu M, Hara A, Okuno M, Matsuno H, Okada K, Ueshima S, et al. Mechanism of Retarded Liver Regeneration in Plasminogen Activator-Deficient Mice: Impaired Activation of Hepatocyte Growth Factor After Fas-Mediated Massive Hepatic Apoptosis. 2001; Available from: https://aasldpubs.onlinelibrary.wiley.com/doi/10.1053/jhep.2001.22650,

18. Kim TH, Mars WM, Stolz DB, Michalopoulos GK. Expression and activation of pro-MMP-2 and pro-MMP-9 during rat liver regeneration. Hepatology [Internet]. 2000 [cited 2023 Oct 24];31(1):75–82. Available from: https://pubmed.ncbi.nlm.nih.gov/10613731/

19. Lee WM. Acetaminophen and the U.S. Acute Liver Failure Study Group: lowering the risks of hepatic failure. Hepatology [Internet]. 2004 Jul [cited 2023 Oct 24];40(1):6–9. Available from: https://pubmed.ncbi.nlm.nih.gov/15239078/

20. Sharma A, Nagalli S. Chronic Liver Disease. Sex/Gender-Specific Medicine in the Gastrointestinal Diseases [Internet]. 2023 Jul 3 [cited 2023 Oct 24];209–27. Available from: https://www.ncbi.nlm.nih.gov/books/NBK554597/

21. Marengo A, Rosso C, Bugianesi E. Liver Cancer: Connections with Obesity, Fatty Liver, and Cirrhosis. Annu Rev Med [Internet]. 2016 Jan 14 [cited 2023 Oct 24];67:103–17. Available from: https://pubmed.ncbi.nlm.nih.gov/26473416/

22. OPTN: Organ Procurement and Transplantation Network - OPTN [Internet]. [cited 2023 Oct 24]. Available from: https://optn.transplant.hrsa.gov/

23. Michalopoulos GK, Bowen WC, Mulè K, Stolz DB. Histological Organization in Hepatocyte Organoid Cultures. Am J Pathol [Internet]. 2001 [cited 2023 Oct 24];159(5):1877. Available from: /pmc/articles/PMC1867077/

24. Sato T, Stange DE, Ferrante M, Vries RGJ, Van Es JH, Van Den Brink S, et al. Long-term expansion of epithelial organoids from human colon, adenoma, adenocarcinoma, and Barrett's epithelium. Gastroenterology [Internet]. 2011 [cited 2023 Oct 24];141(5):1762–72. Available from: https://pubmed.ncbi.nlm.nih.gov/21889923/

25. Zhao Z, Chen X, Dowbaj AM, Sljukic A, Bratlie K, Lin L, et al. Organoids. Nature Reviews Methods Primers 2022 2:1 [Internet]. 2022 Dec 1 [cited 2023 Oct 24];2(1):1–21. Available from: https://www.nature.com/articles/s43586-022-00174-y

26. Asrani SK, Devarbhavi H, Eaton J, Kamath PS. Burden of liver diseases in the world. J Hepatol [Internet]. 2019 Jan 1 [cited 2023 Oct 24];70(1):151–71. Available from: https://pubmed.ncbi.nlm.nih.gov/30266282/

27. Rapid rise in deaths from liver disease in the US over the last decade | BMJ [Internet]. [cited 2023 Oct 24]. Available from: https://www.bmj.com/company/newsroom/rapid-rise-in-deaths-from-liver-disease-in-the-us-over-the-last-decade/

28. Cheemerla S, Balakrishnan M. Global Epidemiology of Chronic Liver Disease. Clin Liver Dis (Hoboken) [Internet]. 2021 May 1 [cited 2023 Oct 24];17(5):365. Available from: /pmc/articles/PMC8177826/

29. Liver Disease | MedlinePlus [Internet]. [cited 2023 Oct 24]. Available from: https://medlineplus.gov/liverdiseases.html

30. Agrawal S, Khazaeni B. Acetaminophen Toxicity. Toxicology Cases for the Clinical and Forensic Laboratory [Internet]. 2023 Jun 9 [cited 2023 Oct 16];75–7. Available from: https://www.ncbi.nlm.nih.gov/books/NBK441917/

31. Brown J, Sorrell JH, McClaren J, Creswell JW. Waiting for a liver transplant. Qual Health Res [Internet]. 2006 Jan [cited 2023 Oct 24];16(1):119–36. Available from: https://pubmed.ncbi.nlm.nih.gov/16317180/

32. Vanholder R, Domínguez-Gil B, Busic M, Cortez-Pinto H, Craig JC, Jager KJ, et al. Organ donation and transplantation: a multi-stakeholder call to action. Nat Rev Nephrol [Internet]. 2021 Aug 1 [cited 2023 Oct 24];17(8):554. Available from: /pmc/articles/PMC8097678/

33. Caplan AL. Finding a solution to the organ shortage. CMAJ. 2016 Nov 1;188(16):1182–3.

34. Abouna GM. Organ Shortage Crisis: Problems and Possible Solutions. Transplant Proc. 2008 Jan;40(1):34–8.

35. Dakhoul L, Gawrieh S, Jones KR, Ghabril M, McShane C, Orman E, et al. Racial Disparities in Liver Transplantation for Hepatocellular Carcinoma Are Not Explained by Differences in Comorbidities, Liver Disease Severity, or Tumor Burden. Hepatol Commun [Internet]. 2018 Jan 1 [cited 2023 Oct 24];3(1):52–62. Available from: https://pubmed.ncbi.nlm.nih.gov/30619994/

36. Nephew LD, Serper M. Racial, Gender, and Socioeconomic Disparities in Liver Transplantation. Liver Transpl [Internet]. 2021 Jun 1 [cited 2023 Oct 24];27(6):900–12. Available from: https://pubmed.ncbi.nlm.nih.gov/33492795/

37. Warren C, Carpenter AM, Neal D, Andreoni K, Sarosi G, Zarrinpar A. Racial Disparity in Liver Transplantation Listing. J Am Coll Surg [Internet]. 2021 Apr 1 [cited 2023 Oct 24];232(4):526–34. Available from: https://pubmed.ncbi.nlm.nih.gov/33444709/

38. Kim WR, Therneau TM, Benson JT, Kremers WK, Rosen CB, Gores GJ, et al. Deaths on the liver transplant waiting list: an analysis of competing risks. Hepatology [Internet]. 2006 Feb [cited 2023 Oct 24];43(2):345–51. Available from: https://pubmed.ncbi.nlm.nih.gov/16440361/

39. Mazari-Arrighi E, Okitsu T, Teramae H, Aoyagi H, Kiyosawa M, Yano M, et al. In vitro proliferation and long-term preservation of functional primary rat hepatocytes in cell fibers. 123AD; Available from: https://doi.org/10.1038/s41598-022-12679-3

40. Zeilinger K, Freyer N, Damm G, Seehofer D, Knö spel F. Cell sources for in vitro human liver cell culture models. Exp Biol Med. 2016;241:1684–98.

41. Yun C, Kim SH, Jung YS. Current Research Trends in the Application of In Vitro Three-Dimensional Models of Liver Cells. 2022; Available from: https://doi.org/10.3390/pharmaceutics15010054

42. Stuart T, Butler A, Hoffman P, Hafemeister C, Papalexi E, Mauck WM, et al. Comprehensive Integration of Single-Cell Data. Cell. 2019 Jun 13;177(7):1888-1902.e21.

43. Tzavlaki K, Moustakas A. TGF-β Signaling. Biomolecules [Internet]. 2020; Available from: www.mdpi.com/journal/biomolecules

44. Hata A, Chen YG. TGF-b Signaling from Receptors to Smads. Available from: http://cshperspectives.cshlp.org/

45. Sun SC. Non-canonical NF-κB signaling pathway. Cell Res [Internet]. 2011;21:71–85. Available from: www.cell-research.com

46. Nakamura T, Mizuno S. The discovery of Hepatocyte Growth Factor (HGF) and its significance for cell biology, life sciences and clinical medicine.

47. Jun-jing Z. PROGRESS IN HEPATOCYTE GROWTH FACTOR RESEARCH. In 2006. Available from: https://api.semanticscholar.org/CorpusID:88323140

48. Zhou B, Lin W, Long Y, Yang Y, Zhang H, Wu K, et al. Notch signaling pathway: architecture, disease, and therapeutics. Signal Transduction and Targeted Therapy 2022 7:1 [Internet]. 2022 Mar 24 [cited 2023 Oct 10];7(1):1–33. Available from: https://www.nature.com/articles/s41392-022-00934-y

49. Patel S, Alam A, Pant R, Chattopadhyay S. Wnt Signaling and Its Significance Within the Tumor Microenvironment: Novel Therapeutic Insights. Front Immunol [Internet]. 2019 Dec 16 [cited 2023 Oct 10];10:2872. Available from: /pmc/articles/PMC6927425/

50. Jun-jing Z. PROGRESS IN HEPATOCYTE GROWTH FACTOR RESEARCH. In 2006. Available from: https://api.semanticscholar.org/CorpusID:88323140

51. Zheng GXY, Terry JM, Belgrader P, Ryvkin P, Bent ZW, Wilson R, et al. Massively parallel digital transcriptional profiling of single cells. Nat Commun [Internet]. 2017 Jan;8:14049. Available from: https://europepmc.org/articles/PMC5241818

52. Zheng GXY, Terry JM, Belgrader P, Ryvkin P, Bent ZW, Wilson R, et al. Massively parallel digital transcriptional profiling of single cells. Nat Commun [Internet]. 2017 Jan 16 [cited 2024 Mar 5];8:14049–14049. Available from: https://europepmc.org/articles/PMC5241818

53. Michalopoulos GK. Hepatostat: Liver regeneration and normal liver tissue maintenance. Hepatology [Internet]. 2017 Apr 1 [cited 2023 Oct 24];65(4):1384–92. Available from: https://pubmed.ncbi.nlm.nih.gov/27997988/

54. Overturf K, Al-Dhalimy M, Ou CN, Finegold M, Grompe M. Serial transplantation reveals the stem-cell-like regenerative potential of adult mouse hepatocytes. Am J Pathol [Internet]. 1997 Nov [cited 2023 Oct 24];151(5):1273. Available from: /pmc/articles/PMC1858091/?report=abstract

55. Azuma H, Paulk N, Ranade A, Dorrell C, Al-Dhalimy M, Ellis E, et al. Robust expansion of human hepatocytes in Fah−/−/Rag2−/−/Il2rg −/− mice. Nat Biotechnol [Internet]. 2007 Aug [cited 2023 Oct 20];25(8):903. Available from: /pmc/articles/PMC3404624/

56. Positive Vs. Negative Selection | Immunomagnetic Cell Separation [Internet]. [cited 2023 Oct 9]. Available from: https://www.stemcell.com/cell-separation/positive-vs-negative-selection

57. Plouffe BD, Murthy SK, Lewis LH. Fundamentals and Application of Magnetic Particles in Cell Isolation and Enrichment. Rep Prog Phys. 2015;

58. Adams JD, Kim U, Tom Soh H. Multitarget magnetic activated cell sorter [Internet]. 2008. Available from: www.pnas.orgcgidoi10.1073pnas.0809795105

59. Kim HO, Huh YJ, Jang J, Choi Y, Kim DW, Kim HS. Selective Depletion of SSEA-3-and TRA-1-60-Positive Undifferentiated Human Embryonic Stem Cells by Magnetic Activated Cell Sorter (MACS). Vol. 8, Tissue Engineering and Regenerative Medicine. 2011.

60. Ito M, Toki K, Hayashi C, Horiguchi A. Hepatocyte Transplantation with Magnet Sorting after Large Hepatectomy for Cholangiocellular Carcinoma [Internet]. 2018. Available from: http://journals.lww.com/transplantjournal

61. Michailidis E, Vercauteren K, Mancio-Silva L, Andrus L, Jahan C, Ricardo-Lax I, et al. Expansion, in vivo-ex vivo cycling, and genetic manipulation of primary human hepatocytes. Proc Natl Acad Sci U S A [Internet]. 2020 Jan 21 [cited 2023 Oct 15];117(3):1678–88. Available from: https://www.pnas.org

62. Grompe M, Lindstedt S, Al-Dhalimy M, Kennaway NG, Papaconstantinou J, Torres-Ramos CA, et al. Pharmacological correction of neonatal lethal hepatic dysfunction in a murine model of hereditary tyrosinaemia type I. Nature Genetics 1995 10:4 [Internet]. 1995 [cited 2023 Oct 15];10(4):453–60. Available from: https://www.nature.com/articles/ng0895-453

63. Grompe M, Lindstedt S, Al-Dhalimy M, Kennaway NG, Papaconstantinou J, Torres-Ramos CA, et al. Pharmacological correction of neonatal lethal hepatic dysfunction in a murine model of hereditary tyrosinaemia type I. Nat Genet [Internet]. 1995 [cited 2023 Oct 20];10(4):453–60. Available from: https://pubmed.ncbi.nlm.nih.gov/7545495/

64. Overturf K, Al-Dhalimy M, Tanguay R, Brantly M, Ou CN, Finegold M, et al. Hepatocytes corrected by gene therapy are selected in vivo in a murine model of hereditary tyrosinaemia type I. Nat Genet [Internet]. 1996 Mar [cited 2023 Oct 20];12(3):266–73. Available from: https://pubmed.ncbi.nlm.nih.gov/8589717/

65. Grompe M, Al-Dhalimy M, Finegold M, Ou CN, Burlingame T, Kennaway NG, et al. Loss of fumarylacetoacetate hydrolase is responsible for the neonatal hepatic dysfunction phenotype of lethal albino mice. Genes Dev [Internet]. 1993 [cited 2023 Oct 20];7(12A):2298–307. Available from: https://pubmed.ncbi.nlm.nih.gov/8253378/

66. Liao J, Lu Q, Li Z, Li J, Zhao Q, Li J. Acetaminophen-induced liver injury: Molecular mechanism and treatments from natural products. 2023;

67. Yang T, Wang H, Wang X, Li J, Jiang L. The Dual Role of Innate Immune Response in Acetaminophen-Induced Liver Injury. Biology (Basel) [Internet]. 2022 Jul 14;11(7). Available from: https://doi.org/10.3390/biology11071057

68. Huang W, Ma K, Zhang J, Qatanani M, Cuvillier J, Liu J, et al. Nuclear receptor-dependent bile acid signaling is required for normal liver regeneration. Science [Internet]. 2006 Apr 14 [cited 2023 Oct 24];312(5771):233–6. Available from: https://pubmed.ncbi.nlm.nih.gov/16614213/

69. Nuciforo S, Heim MH. Organoids to model liver disease. Vol. 3, JHEP Reports. Elsevier B.V.; 2021.

70. Bonkovsky HL, Jones DP, Russo MW, Shedlofsky SI. Chapter 25 - Drug-Induced Liver Injury. In: Boyer TD, Manns MP, Sanyal AJ, editors. Zakim and Boyer's Hepatology (Sixth Edition) [Internet]. Sixth Edition. Saint Louis: W.B. Saunders; 2012. p. 417–61. Available from: https://www.sciencedirect.com/science/article/pii/B9781437708813000255

71. Liao J, Lu Q, Li Z, Li J, Zhao Q, Li J. Acetaminophen-induced liver injury: Molecular mechanism and treatments from natural products. 2023.

72. Huang HL, Wang YJ, Zhang QY, Liu B, Wang FY, Li JJ, et al. Hepatoprotective effects of baicalein against CCl4-induced acute liver injury in mice. World J Gastroenterol. 2012;18(45):6605–13.

73. Nuciforo S, Heim MH. Organoids to model liver disease. Vol. 3, JHEP Reports. Elsevier B.V.; 2021.

74. Lo RC, Kim H. Histopathological evaluation of liver fibrosis and cirrhosis regression. Vol. 23, Clinical and Molecular Hepatology. Korean Association for the Study of the Liver; 2017. p. 302–7.

75. Kang SH, Kim MY, Eom YW, Baik SK. Mesenchymal stem cells for the treatment of liver disease: Present and perspectives. Vol. 14, Gut and Liver. Editorial Office of Gut and Liver; 2020. p. 306–15.

76. Power C, Rasko JEJ. Annals of Internal Medicine History of Medicine Whither Prometheus ' Liver ? Greek Myth and the Science of Regeneration. Ann Intern Med. 2008;149(6).

77. Fausto N. Liver regeneration and repair: Hepatocytes, progenitor cells, and stem cells. Vol. 39, Hepatology. 2004.

78. Elaut G, Henkens T, Papeleu P, Snykers S, Vinken M, Vanhaecke T, et al. Molecular Mechanisms Underlying the Dedifferentiation Process of Isolated Hepatocytes and Their Cultures. Curr Drug Metab. 2006;7(6).

79. Zeilinger K, Freyer N, Damm G, Seehofer D, Knöspel F. Cell sources for in vitro human liver cell culture models. Exp Biol Med. 2016;241(15).

80. Funk C, Roth A. Current limitations and future opportunities for prediction of DILI from in vitro. Vol. 91, Archives of Toxicology. 2017.